REVIEW

Construction and demolition waste repurposed for heavy metal ion removal from wastewater: a review of current approaches

K. H. Ranaweera[1] · M. N. C. Grainger[1] · A. D. French[2] · M. R. Mucalo[1]

Abstract

Over the past few decades, the world is facing critical water supply problems caused by the relentless increase of global human populations and the associated rise of anthropogenic activities. Heavy metals are among the main water pollutants which pose a great threat to human health. Hence, globally there has been a large amount of research devoted to investigating cost-effective and sustainable methods for removal of heavy metals from polluted water. One such area of interest is the utilization of construction and demolition waste (CDW) materials for the adsorptive removal of heavy metal ions (As, Cd, Co, Cr, Cu, Hg, Ni, Pb, Sr, and Zn). This review focuses on the most current research for the use of CDW as an adsorbent. The different heavy metal ion removal mechanisms involved are also discussed. Further, this article documents the regeneration and reuse strategies for heavy metal treated adsorbents and the efforts to apply these materials in large-scale applications. Finally, the main research gaps are identified and future research directions suggested.

Introduction

Water can be considered as one of the prime natural resources for which maintenance of quality is mandatory for the survival of living beings (Chaplin 2006). Apart from its obvious involvement in bodily functions, water is essential for many other applications, specifically in the industrial, electrical, and agricultural sectors. Hence, the unaddressed contamination of water on the planet has serious repercussions for global populations.

Water pollution is defined as any change in the physical, chemical, or biological properties of the water that is harmful to living beings (Helmer and Hespanhol 1997). Water can become contaminated with pollutants relatively easily because it is a universal solvent for many substances: organic chemicals, dyes, fertilizers (higher amounts of nitrates and phosphates), heavy metals (common examples include As, Cd, Cr, Cu, Hg, Pb, and Zn), chlorinated solvents, pesticides, solid particles, and infectious microorganisms. All of these can dissolve in water and thus contaminate it (Gambhir et al. 2012).

Heavy metals (As, Cd, Cr, Cu, Hg, Ni, Pb, Zn, etc.) are elements that have a high density (greater than 5 g/cm^3). These metals are non-biodegradable, highly bio-accumulative, and difficult to eliminate naturally from the environment (Murugesan et al. 2006). Heavy metals have both natural and anthropogenic origin. Natural origins include erosion of sediments, soil weathering, and volcanic activity, while anthropogenic origins include activities such as mining, processing, and industrial wastewater discharge (Lata et al. 2015; Davy and Trompetter 2018).

Heavy metal contamination in water has been reported throughout the world, including in Nigeria (Oyeku 2010), Bangladesh (Mohiuddin et al. 2011), Turkey (Varol and Şen 2012), India (Singh and Kumar 2006), Pakistan (Rasool et al. 2016), and Canada (McGuigan et al. 2010). It has been reported that chronic heavy metal poisoning affects millions of people, and that each year, 1.6 million children die from diseases caused due to contaminated drinking water

✉ M. R. Mucalo
michael.mucalo@waikato.ac.nz

1   School of Science, University of Waikato, Hamilton 3240, New Zealand

2   Pacific Northwest National Laboratory, Richland, WA 99354, USA

🖐 ☺ Springer

(Fernandez-Luqueno et al. 2013). As heavy metals have been proven to show toxicological effects even at very low concentrations, organizations such as the World Health Organization (WHO) have set permissible exposure limits of these contaminants in drinking water (see Table 1).

Given the dangers of heavy metal pollution in water supplies, there is thus a strong incentive to try and remove these pollutants. There are various procedures that are available such as adsorption, reverse osmosis, chemical precipitation, ion exchange, and ultrafiltration (Ahalya et al. 2003). Adsorption is reasoned to be one of the best pollution control technologies to use for heavy metal treatment because of its low cost, easy operation, and high efficiency (Senthil Kumar et al. 2013). Moreover, adsorbents can be regenerated via a desorption process on some occasions as the adsorption is often a reversible reaction (Burakov et al. 2018). Another advantage is that various natural or waste materials could be considered as potential adsorbents which means that there is an opportunity to repurpose superfluous by-products, which will reduce waste sent to landfill. Therefore, evaluation of the adsorption potential of different types of waste materials such as agricultural waste, industrial waste, and CDW for heavy metal treatment has become an emerging research area (Amin et al. 2006; Amarasinghe and Williams 2007; Labidi 2008; Hua et al. 2015; Bayuo et al. 2019; Krishnamoorthy et al. 2019; Kumara et al. 2019). The effectiveness of an adsorption process is evaluated by performing batch and column adsorption studies. Isothermal adsorption studies and adsorption kinetic studies are performed to explain and to delve more deeply into the mechanisms involved with the process.

Batch adsorption process

In batch mode adsorption, the same adsorbate solution remains in contact with the adsorbent until equilibrium is established. The isotherm models that are discussed in this article are briefly explained below.

Table 1 The World Health Organization (WHO) drinking water maximum permissible exposure levels for heavy metals (WHO 2011)

Heavy metal	Maximum permissible exposure level (mg/L)
Arsenic (As)	0.01
Cadmium (Cd)	0.003
Chromium (Cr)	0.05
Copper (Cu)	2.0
Lead (Pb)	0.01
Mercury (Hg)	0.006
Nickel (Ni)	0.07

- Langmuir isotherm model

The Langmuir isotherm model is based on the assumption that the adsorbate adsorbs onto localized active sites present on the adsorbent surface and that the adsorbent possesses active sites, which are energetically equivalent, having the same affinity for adsorbates to form a monolayer, that no interaction occurs between adsorbed molecules, and adsorption approaches equilibrium between the adsorbate in the solution and the adsorbate adsorbed on to the adsorbent. The nonlinearized form of the Langmuir isotherm model is given by Eq. (1) (Langmuir 1918).

$$q_e = \frac{q_m b C_e}{1 + b C_e} \tag{1}$$

where q_e denotes the amount of solute adsorbed per unit mass of adsorbent at equilibrium (mg g^{-1}), q_m is the amount of solute required to form a complete monolayer (mg g^{-1}), C_e is the residual liquid phase concentration at equilibrium (mg dm^{-3}), and b is the adsorption coefficient or Langmuir equilibrium constant which is related to the binding energy or affinity parameter of the adsorption system (dm^3 mg^{-1}) (Wong et al. 2003; Ghosal and Gupta 2017).

- Freundlich isotherm model

The multilayer adsorption of an adsorbate on a heterogeneous surface of an adsorbent in aqueous medium is explained by the Freundlich isotherm model (Poorkarimi et al. 2013). The nonlinearized form of the Freundlich isotherm model is given by Eq. (2) (Freundlich 1906).

$$q_e = K C_e^{1/n} \tag{2}$$

where K and $1/n$ are Freundlich isotherm constants. $1/n$ (heterogeneity factor) is related to the adsorption intensity and adsorption capacity is implied by K (Olalekan et al. 2013).

- Redlich–Peterson isotherm

The Redlich–Peterson isotherm combines elements of both the Freundlich and Langmuir isotherm models and is represented by Eq. (3) (Redlich and Peterson 1959).

$$q_e = \frac{a C_e}{1 + b C_e^n} \tag{3}$$

where a (L g^{-1}) and b (L mg^{-1}) are constants, and n is an exponent which lies between 0 and 1 (Maji et al. 2007).

- Koble–Corrigan isotherm model

The Koble–Corrigan isotherm model is a three-parameter isotherm model which is represented by Eq. (4). This isotherm model also incorporates both Freundlich and Langmuir isotherm models for representation of adsorption data at equilibrium (Koble and Corrigan 1952).

$$\frac{1}{q_e} = \left(\frac{1}{A_k C_e^p}\right) + \frac{B_k}{A_k} \tag{4}$$

where A_k, B_k, p are Koble–Carrigan's isotherm constants (Ayawei et al. 2017).

- Radke–Prausnitz isotherm

The Radke–Prausnitz isotherm model is explained by Eq. (5). This model reduces to a linear form at low initial metal ion concentrations and becomes the Freundlich isotherm model at high adsorbate concentrations (Radke and Prausnitz 1972).

$$q_e = \frac{q_{MRP} K_{RP} C_e}{\left(1 + K_{RP} C_e\right)^{MRP}} \tag{5}$$

where K_{RP} is the Radke–Prausnitz equilibrium constant, q_{MRP} is the Radke–Prausnitz maximum adsorption capacity (mg g^{-1}), and MRP is the Radke–Prausnitz model exponent (Ayawei et al. 2017).

- Dubinin–Radushkevich (D-R) isotherm

The D-R isotherm model is based on the assumption that adsorption in micropores is pore filling rather than via layer by layer surface coverage (Hutson and Yang 1997). This model is represented by Eq. (6) (Radushkevich 1947).

$$q_e = q_m \exp{-\beta \varepsilon^2} \tag{6}$$

where β is a constant related to the mean free energy of adsorption (mol^2 J^{-2}) and ε is the Polanyi potential which is given by Eq. (7).

$$\varepsilon = RT \ln\left(1 + \frac{1}{C_e}\right) \tag{7}$$

where R is the universal gas constant (J K^{-1} mol^{-1}) and T is the absolute temperature (K) at equilibrium (Inyinbor et al. 2016).

- Brunauer–Emmettt–Teller (BET) isotherm model

The BET theory extends the Langmuir model to multilayer adsorption scenarios and assumes adsorption occurs on a homogenous surface with no lateral interaction between molecules, and on one binding site per molecule/

adsorbate where multiple molecules can get adsorbed with different affinities. This model is represented by (Brunauer et al. 1938);

$$q_e = \frac{q_s C_{BET} C_e}{\left(C_s - C_e\right)\left[1 + \left(C_{BET} - 1\right)\right]\left[\frac{C_e}{C_s}\right]} \tag{8}$$

where C_s is the adsorbate monolayer saturation concentration (mg L^{-1}), q_s is the theoretical isotherm saturation capacity (mg g^{-1}), and C_{BET} is a constant relating to the energy of surface interaction (Itodo et al. 2018).

The kinetic models for adsorption processes that are discussed in this article are as follows.

- Pseudo-first-order kinetic model

This model is based on the assumption that the rate-limiting step in the adsorption depends on the collisions between adsorbates with vacant single sites on the adsorbent surface. This model is illustrated by Eq. (9) (Lagergren 1898).

$$q_t = q_e\left(1 - e^{-k_1 t}\right) \tag{9}$$

where k_1 (min^{-1}) is the equilibrium rate constant of pseudo-first-order adsorption, q_e is the amount adsorbed on to the adsorbent surface at equilibrium (mg g^{-1}), and q_t is the adsorption capacity at time t (mg g^{-1}).

- Pseudo-second-order kinetic model

The pseudo-second-order kinetic model which (Eq. 10) is based on the assumption that the rate-limiting step is chemisorption involving valency forces through exchange or sharing of electrons between the adsorbent and adsorbate as ion exchange and covalent forces (Blanchard et al. 1984).

$$q_t = \frac{k_2 q_e^2 t}{1 + k_2 q_e t} \tag{10}$$

where k_2 is the rate constant for pseudo-second-order adsorption (g mg^{-1} min^{-1}).

- Elovich kinetic model

The Elovich kinetic model (Eq. 11) assumes that the solute adsorption rate exponentially decreases as the adsorbed solute amount increases (Elovich and Larinov 1962).

$$\frac{dq_t}{dt} = \alpha e^{-\beta q_t} \tag{11}$$

where α is the initial sorption rate (mg g^{-1} min^{-1}) and β is related to the activation energy for chemisorption and the extent of surface coverage (g mg^{-1}) (Riahi et al. 2017).

- Bangham kinetic model

This model assumes that the only rate-controlling step in the adsorption process is pore diffusion. It is suggested that the adsorption process mainly occurs at the surface of the adsorbent and only slightly in internal pores (Ghazy and Gad 2014; Yokogawa et al. 2017). This model is represented by Eq. (12) (Aharoni et al. 1979).

$$\log \left\{ \log \left(\frac{C_b}{C_b - q_t m} \right) \right\} = \log \left(\frac{k_o m}{2.303 V} \right) + \sigma \log (t) \tag{12}$$

where m is adsorbent amount (g), C_b is initial liquid phase adsorbate amount (mg), V is used solution volume (L), and k_o (L g^{-1}) and σ (< 1) are both Bangham equation parameters (Barkakati et al. 2010).

Fixed-bed adsorption process

In fixed-bed adsorption, the influent solution continuously flows through the column packed with the adsorbent. The fixed-bed column modelling of CDW-derived adsorbents has been performed by using models such as the Adam–Bohart model and Yan model.

- Adam–Bohart model

This model assumes that the rate of adsorption is proportional to the residual capacity of the adsorbent and the concentration of the adsorbate. It is illustrated in nonlinear form as (Bohart and Adams 1920);

$$\frac{C_t}{C_o} = e^{K_{AB} C_o t - K_{AB} N_o \frac{H}{u}} \tag{13}$$

where C_t and C_o are effluent and influent concentrations, respectively (mg L^{-1}), K_{AB} is the Bohart–Adams rate constant (L mg^{-1} h^{-1}), N_0 is the saturation concentration of the column (mg L^{-1}), H is the packed column depth (cm), t is the flow time (h) and u is the flow rate per unit cross-sectional area (cm h^{-1}).

- Yan model

The Yan model is represented by Eq. (14) and it was developed for the purpose of minimizing the errors resulting from the Thomas model which is another model used to model the column adsorption process (Yan et al. 2001; Chittoo and Sutherland 2020).

$$\frac{C_t}{C_o} = 1 - \frac{1}{1 + \left[\frac{Q^2 t}{K_Y} q_Y m \right]^{\left(\frac{K_Y C_o}{Q} \right)}} \tag{14}$$

where m is mass of the adsorbent packed in the column (g), q_Y is the maximum capacity of adsorption (mg g^{-1}), K_Y is Yan's rate constant (L mg^{-1} h^{-1}), and Q is the flow rate (L h^{-1}).

Definition of construction and demolition waste

Construction waste is defined as waste from construction, remodelling, and repair of individual residences, commercial buildings and other structures. Demolition waste is defined as waste generated from razed buildings and other structures (Tchobanoglous et al. 1993). Table 2 summarizes the composition of CDW in a selected number of countries or large urban centres.

Construction practices differ from country to country. For instance, concrete, steel, and wood are the most widely used construction materials on the North American continent,

Table 2 CDW composition in several countries/urban centres of varying populations

Country/Region	Population (Million)	Year	% composition of CDW						References
			Concrete and bricks	Wood	Glass	Plastic	Metal	Other (Paper, Textile, Hazardous etc.)	
Dhaka-Capital of Bangladesh	8.5	2016	81	3	0.6	0.6	3	11.8	Islam et al. (2019)
Mainland Portugal	10.6	2012	35	5	2	1	5	52	Tonini et al. (2018), Passos et al. (2020)
New Zealand	4.2	2007	25	38	1	1	6	29	Inglis (2007)
Norway	4.5	2002	67.24	14.58	0.26	N/A	3.63	14.29	Keilman et al. (2002), Bergsdal et al. (2007)
Tehran-Capital of Iran	8.4	2011–2016	37	0.51	1	N/A	0.7	60.79	Asgari et al. (2017)
United States	319	2014	67	7	>1	>1	1	23	Townsend et al. (2014), Colby and Ortman (2015)

whereas in Europe the main construction materials are concrete and masonry (Khan 2016). The most commonly used wood products in the USA include softwood lumber, engineered wood, plywood, and oriented strand board (McKeever and Elling 2015). The use of wood in the construction sector is highly limited in Europe. Asian countries mostly utilize baked clay, stone masonry, and concrete for construction (Okazaki et al. 2012). Currently, New Zealand and Australia mostly use engineered wood products for construction which mainly include laminated veneer lumber, glue-laminated timber, and cross-laminated timber. Along with engineered wood products, concrete, steel, and plasterboard are also being used in the construction sector of these countries (Evison et al. 2018).

Resource recovery from CDW materials and improvements towards a circular economy (CE) are becoming a fast-growing research area recently (Kirchherr et al. 2017). Currently, the main application of the CE concept for CDW management is recycling and repurposing these materials into construction materials (del Río Merino et al. 2010; Schwerin et al. 2013; Adamopoulos et al. 2015; Ndukwe and Yuan 2016; Menegaki and Damigos 2018; Risse et al. 2019). However, it is beneficial to find alternative uses for CDW outside the construction industry; one potential application of these materials is the investigation of these materials as adsorbents for the removal of pollutants from aqueous solutions (Caicedo et al. 2020). Improvements in utilizing CDW as adsorbents will be beneficial to contribute towards attaining a "zero-waste society" in the future especially if they can be regenerated for repeated use in this application.

Herein, we review and summarize the latest research advancements into the application of CDW for heavy metal ion treatment. The specific objectives of this review are as follows: (i) to report the adsorbents developed from CDW for heavy metal ion treatment, factors influencing the adsorption process, heavy metal ion removal mechanisms, and comparison of their adsorption capacities, (ii) to evaluate existing regeneration methods for the treated adsorbents, (iii) to investigate the current research efforts towards industrial scale applications of the CDW-derived adsorbents, and (iv) to provide possible future prospects for how further developments in this field can be advanced.

CDW as adsorbents for heavy metal ion treatment

CDW has been used for heavy metal treatment in the form of either direct application as an adsorbent or after modification by different treatment methods such as activated carbon production, biochar production, and chemical modification (Argun et al. 2007; Ghazy et al. 2008; Rafatullah et al. 2009, 2012; Salim and Munekage 2009a, b; Ghazy and Gad 2014; Yoo et al. 2018; Wu et al. 2019; Herath et al. 2021). Figure 1 summarizes the different methods utilized in the application

of CDW as adsorbents for heavy metal remediation. The experimental results of the studies which used CDW directly for heavy metal ion treatment are summarized in Table 3.

Direct application of CDW-derived adsorbents for heavy metal ion treatment

Concrete

Concrete waste is generated in large amounts every year, as it is globally one of the most widely used materials. Concrete waste is generated in several forms: concrete sludge, demolished concrete, and fine concrete waste (Ho et al. 2020). Several adsorption studies have been conducted using various types of concrete CDW with varying results.

Concrete sludge is a slurried industrial waste consisting of aggregates, hydrated cement, and water. Yoo et al. studied the removal of Pb(II), Cu(II), and Zn(II) utilizing dried concrete sludge (<25 μm particle size fraction), which primarily consisted of muscovite ($KAl_2(Si_3AlO_{10})(OH)_2$), quartz ($SiO_2$), and albite ($NaAlSi_3O_8$), and obtained percentage removal values of 99.9%, 98.3%, and 95.2%, respectively, during 1440 min (Yoo et al. 2018).

Ali et al. performed a similar study using demolished concrete (1–2 mm fraction) as an adsorbent for removal of Pb(II), Cu(II), and Ni(II) ions from a synthetic wastewater sample. Both batch and column adsorption studies were performed to evaluate the adsorption potential of the demolished concrete. According to energy-dispersive X-ray (EDX) analysis, Al, Ca, Fe, K, Mg, Na, S and Si were identified as the major components of the adsorbent. Maximum adsorption capacities of 86.297, 39.286, and 13.560 mg g^{-1} have been obtained for Pb(II), Cu(II), and Ni(II) ions, respectively, after 180 min of exposure (Ali and Abd Ali 2020).

The generation of fine concrete waste residues during the production of autoclaved aerated concrete (AAC) is unavoidable (Bao et al. 2016). AAC is a highly porous, lightweight wall material consisting of SiO_2, tobermorite ($Ca_5Si_6O_{16}(OH)_2 \cdot 4H_2O$), anhydrite ($CaSO_4$), and gypsum ($CaSO_4 \cdot 2H_2O$) (Jerman et al. 2013; Kumara et al. 2019). Several studies have reported its potential as a water treatment matrix. A study has been carried out by Kumara et al. for sequestering Cd(II) and Pb(II) ions using AAC. The adsorbent was characterized using X-ray diffraction (XRD), Brunauer–Emmett–Teller (BET), and EDX analysis. The effects of parameters such as particle size, initial metal ion concentration, ionic strength, initial pH, contact time, and the presence of competitive metals were studied. The adsorption behaviour for both Cd(II) and Pb(II) ions followed the pseudo-second-order kinetic model and Langmuir isotherm model at initial metal ion concentrations at or below 2000 mg L^{-1} with higher initial metal ion concentrations following the Freundlich isotherm model. This
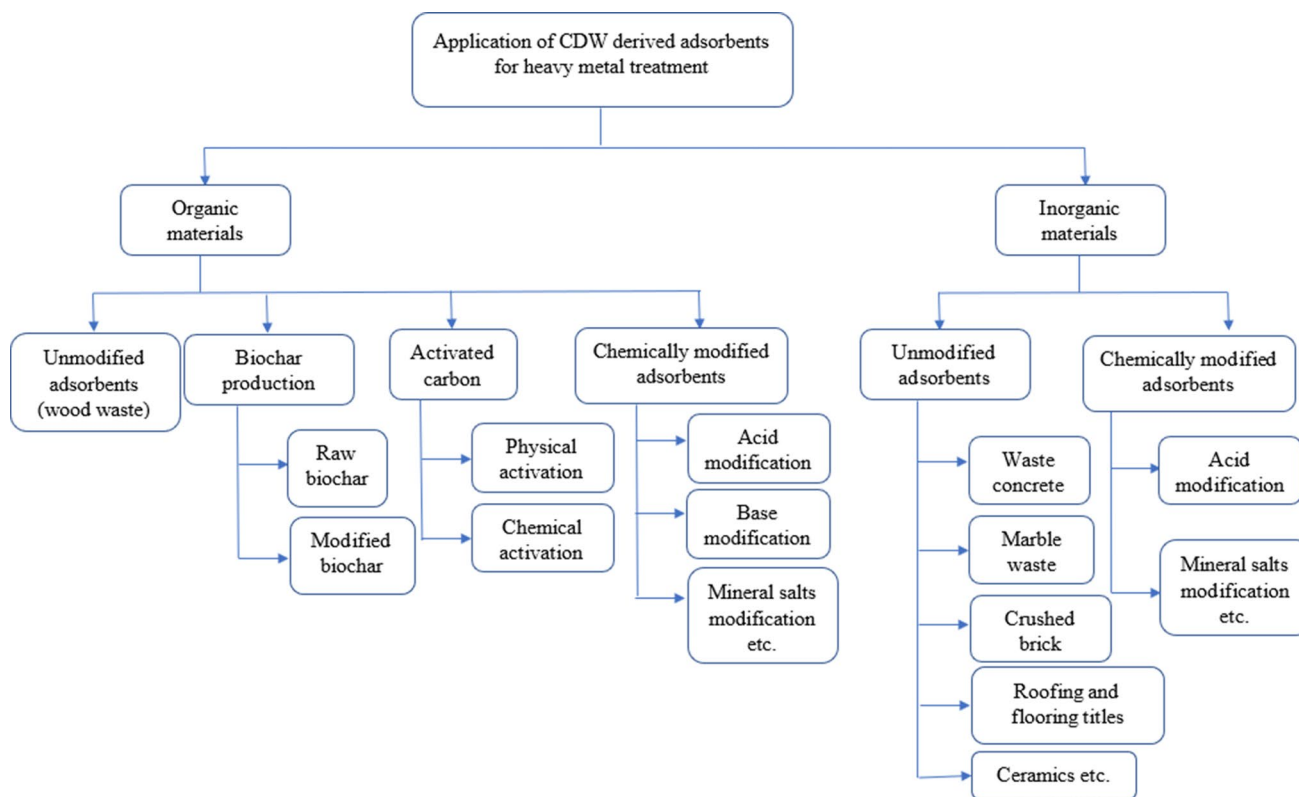
Fig. 1 Summary of different methods utilized in the application of CDW as adsorbents reported in the literature (Argun et al. 2007; Ghazy et al. 2008; Rafatullah et al. 2009, 2012; Salim and Munekage 2009a, b; Ghazy and Gad 2014; Yoo et al. 2018; Wu et al. 2019; Herath et al. 2021)

suggested that monolayer adsorption behaviour shifts to multilayer adsorption on exposure of the adsorbent to higher metal ion concentrations (Kumara et al. 2019). Based on the experimental results of previous studies, concrete has been shown to be useful for the adsorption of Cd(II), Cu(II), Ni(II), Pb(II), and Zn(II) ions under various adsorption conditions.

Marble waste

Marble dust is a by-product produced during marble processing which has been previously tested as an adsorbent. Ghazy et al. studied the potential of the powdered marble waste obtained from the marble processing workshops as an adsorbent for the removal of Pb(II) ions from aqueous solutions. The marble samples used as adsorbents consisted of 60% $CaCO_3$ and 6% $MgCO_3$, with the remainder being composed of SiO_2, feldspar, clays, pyrite, and siderite. Both Langmuir and Freundlich isotherm models fit well with the experimental data, and the sorption capacity of the adsorbent was reported as 101.6 mg g^{-1} (Ghazy and Gad 2014).

A similar study was performed to evaluate the marble waste adsorption potential towards Cd(II) ions. A maximum adsorption capacity of 30.92 mg g^{-1} was obtained based on the adsorption isothermal studies, and it was found that

the Langmuir and Freundlich adsorption isotherms best described the adsorption process. Ion exchange, precipitation, and chemical interaction were identified as the main mechanisms of Cd(II) ion removal (Ghazy et al. 2008). Marble waste was also used to treat arsenic. The adsorption process was best explained by the Langmuir model with a maximum monolayer adsorption capacity of 0.04 mg g^{-1}. Based on the SEM analysis of the materials studied, the adsorbent possesses an uneven surface structure with a large number of pores, which can provide active sites for binding of adsorbate either physically or chemically (Bibi et al. 2015).

The experimental results of these studies indicate that marble waste has the potential for the removal of heavy metal ions. The sorption capacity values have changed in a wide range (0.04–101.6 mg g^{-1}) for the studied metal ions. One of the factors that may have caused this is the wide range of the studied initial concentrations (Arsenic: 0.1–1 mg L^{-1}, Cd(II): 20–60 mg L^{-1}, Pb(II): 500–1500 mg L^{-1}). Previous studies report that metal ion adsorption capacity increases with increasing initial metal ion concentrations due to factors such as a higher probability of collisions between the adsorbents and metal ions and enhanced driving force of metal ions diffusion onto the adsorbent surface (Putra et al. 2014; Ouyang et al. 2019). The nature of the metal ions (electronegativity and hydrated ionic radii) can be suggested

Table 3 Direct application of construction and demolition waste in heavy metal ion treatment as reported in the literature

Adsorbate (ionic species)	Adsorbent	Adsorbent properties (Surface area (m² g⁻¹), average pore diameter (nm), particle size (mm), average pore volume (cm³ g⁻¹))	Adsorption capacity (mg/g)	Characterization method	Adsorption technique (Batch/Column) and conditions (Dosage (g/g L⁻¹), Concentration (mg L⁻¹), Temperature (°C), pH, Agitation speed (rpm), Contact time (min), Bed depth (cm), flowrate (mL min⁻¹))	Isotherm model which best explain the adsorption behaviour	Kinetic model which best explain the adsorption behaviour	References
Inorganic materials								
As(III)-based ions	Marble waste	0.05 mm	0.04	XRD, SEM	Batch (10–40 g, 0.1–1 mg L⁻¹, 30–90 min, 150 rpm)	Langmuir	N/A	Bibi et al. (2015)
	Brick	<0.3 mm	0.04	XRD, SEM	Batch (10–40 g, 0.1–1 mg L⁻¹, 30–90 min, 150 rpm)	Langmuir	N/A	Bibi et al. (2015)
	Silica ceramic	0.42±0.02 mm, 211.657 m² g⁻¹, 4.9446 nm, 0.2616 cm³ g⁻¹	1.789	SEM, BET	Batch (10–100 g L⁻¹, 20–98 mg L⁻¹, 0–3600 min, pH: 4–10.7, 150 rpm, 15–45 °C)	Freundlich	Pseudo-second-order	Salim and Munekage (2009a, b)
Cd(II) ions	AAC	<0.105, 0.105–2, 2–4.75 mm, 23.6, 23.6, 21.9 m² g⁻¹	16.5	XRD, SEM/EDX, BET	Batch (100 g L⁻¹ or 16.7 g L⁻¹, 0–5000 mg L⁻¹, 60–11,520 min, 100 rpm, 25)	Langmuir	Pseudo-second-order	Kumara et al. (2019)
	Laterite	<0.105, 0.105–2 mm	N/A	N/A	Batch (25 °C, 25–900 mg L⁻¹, 1440 min, 100 rpm)	Freundlich	N/A	Hai et al. (2018)
	Marble waste	0.025–0.063 mm, 21.8 m² g⁻¹, 0.98 cm³ g⁻¹, 1.89 nm	30.92	FTIR, BET	Batch (20–60 mg L⁻¹, 2 g L⁻¹, 650 rpm, 1–300 min, 25–45 °C)	Langmuir and Freundlich	N/A	Ghazy et al. (2008)
Co(II) ions	Roof tiles	0.3–0.6 mm	3.83	XRD, FTIR	Batch (5 g L⁻¹, 10 rpm, 15–1728 min, ~6–472 mg L⁻¹)	Freundlich	Pseudo-second-order	Jelić et al. (2017)
Cu(II) ions	Demolished concrete	1–2 mm, 11.0956 m² g⁻¹	39.286	SEM, EDX, BET	Column (5–15 cm, 5 mL min⁻¹); Batch (50–3000 g L⁻¹, 100–750 mg L⁻¹, 0–300 min, 0–250 rpm)	Yan Langmuir and Radke–Prausnitz	N/A	Ali and Abd Ali (2020)
	Concrete sludge	<0.025 mm, 23.1 m² g⁻¹	N/A	SEM, XRD, BET	Batch (10–1 g L⁻¹, 0–1440 min, 30 rpm, pH:1–5)	N/A	N/A	Yoo et al. (2018)
	Brick	2–5 mm, 1.75 m² g⁻¹, 0.0051 cm³ g⁻¹, 12.00 nm	0.5 mg L⁻¹–0.088, 1.0 mg L⁻¹–0.104, 2.0 mg L⁻¹–0.1696	SEM, XRF, BET, FTIR	Column (5–20 cm, 0.5–2 mg L⁻¹)	Adams-Bohart	N/A	Zhang et al. (2019)

Table 3 (continued)

Adsorbate (ionic species)	Adsorbent	Adsorbent properties (Surface area ($m^2\ g^{-1}$), average pore diameter (nm), particle size (mm), average pore volume ($cm^3\ g^{-1}$))	Adsorption capacity (mg/g)	Characterization method	Adsorption technique (Batch/Column) and conditions (Dosage ($g/g\ L^{-1}$), Concentration ($mg\ L^{-1}$), Temperature (°C), pH, Agitation speed (rpm), Contact time (min), Bed depth (cm), flowrate ($mL\ min^{-1}$))	Isotherm model which best explain the adsorption behaviour	Kinetic model which best explain the adsorption behaviour	References
Hg(II) ions	Brick	0.1–1 mm	87	XRD	Batch (2–$20\ g\ L^{-1}$, 100–$500\ mg\ L^{-1}$, 0–400 min, pH: 1.5–6, 3500 rpm)	Langmuir	N/A	Labidi (2008)
Ni(II) ions	Demolished concrete	1–2-mm, 11.0956 $m^2\ g^{-1}$	13.560	SEM, EDX, BET	Column (5–15 cm, $5\ mL\ min^{-1}$)	Yan Langmuir and Radke–Prausnitz	N/A	Ali and Abd Ali (2020)
	Roof tiles	0.3–0.6 mm	5.87	XRD, FTIR	Batch (50–$3000\ g\ L^{-1}$, 100–$750\ mg\ L^{-1}$, 0–300 min, 0–250 rpm)	Freundlich	Pseudo-first-order	Jelić et al. (2017)
Pb(II) ions	Concrete sludge	<0.025 mm, 23.1 $m^2\ g^{-1}$	N/A	SEM, XRD, BET	Batch (10–$1\ g\ L^{-1}$, 0–1440 min, 30 rpm, pH:1–5)	N/A	N/A	Yoo et al. (2018)
	AAC	<0.105, 0.105–2, 2–4.75 mm, 23.6, 23.6, 21.9 $m^2\ g^{-1}$	>250	XRD, SEM/EDX, BET	Batch ($10.0\ g\ L^{-1}$ or $16.7\ g\ L^{-1}$, 0–$5000\ mg\ L^{-1}$, 60–$11{,}520$ min, 100 rpm, 25 °C)	Langmuir and Freundlich	Pseudo-second-order	Kumara et al. (2019)
	Marble waste	0.025–0.063 mm, 21.8 $m^2\ g^{-1}$, 0.98 $cm^3\ g^{-1}$, 1.89 nm	101.6	FTIR, BET, XRD	Batch ($1\ g\ L^{-1}$, 500–$1500\ mg\ L^{-1}$, 1–20 min and 25–135 min, 270 rpm, pH 2–10, 25–45 °C)	Langmuir and Freundlich	Bangham	Ghazy and Gad (2014)
	Demolished concrete	1–2-mm, 11.0956 $m^2\ g^{-1}$	86.297	SEM, EDX, BET	Batch (50–$3000\ g\ L^{-1}$, 100–$750\ mg\ L^{-1}$, 0–300 min, 0–250 rpm) Column (5–15 cm, $5\ mL\ min^{-1}$)	Langmuir and Radke–Prausnitz Yan	N/A	Ali and Abd Ali (2020)
	Silica ceramic	<0.05 mm, 340.38 $m^2\ g^{-1}$, 4.446 nm, 0.3274 $cm^3\ g^{-1}$	2.7	SEM, BET	Batch (5–$40\ g\ L^{-1}$, 10–$50\ mg\ L^{-1}$, pH: 2.45–11.5, 140 rpm, 20–40 °C)	Langmuir	Pseudo-second-order	Salim and Munekage (2009a, b)
Sr(II) ions	Roof tile	0.3–0.6 mm	2.63	XRD, FTIR	Batch ($5\ g\ L^{-1}$, 10 rpm, 15–1728 min, 9–$701\ mg\ L^{-1}$)	Freundlich	Pseudo-second-order	Jelić et al. (2017)

Table 3 (continued)

Adsorbate (ionic species)	Adsorbent	Adsorbent properties (Surface area ($m^2\,g^{-1}$), average pore diameter (nm), particle size (mm), average pore volume ($cm^3\,g^{-1}$)	Adsorption capacity (mg/g)	Characterization method	Adsorption technique (Batch/Column) and conditions (Dosage (g/g L^{-1}), Concentration (mg L^{-1}), Temperature (°C), pH, Agitation speed (rpm), Contact time (min), Bed depth (cm), flowrate (mL min^{-1}))	Isotherm model which best explain the adsorption behaviour	Kinetic model which best explain the adsorption behaviour	References
Zn(II) ions	Concrete sludge	<0.025 mm, 23.1 $m^2\,g^{-1}$	N/A	SEM, XRD, BET	Batch (10–1 g L^{-1}, 0–1440 min, 30 rpm, pH:1–5)	N/A	N/A	Yoo et al. (2018)
	M-brick	0.045–0.15, 2–4.760 mm, 1.2655 $m^2\,g^{-1}$(0.595–1.190 mm)	3.9	XRD, SEM, BET, XRF	Batch (10 g L^{-1}, 40–90 mg L^{-1}, 0–1440 min, 100 rpm, 25±2 °C, pH: 2.5, 4.5, 7)	Redlich–Peterson	Elovich	Arabyarmohammadi et al. (2014)
	H-bricks	0.045–0.15, 2–4.760 mm, 0.3317 $m^2\,g^{-1}$ (0.595–1.190 mm)	2.45	XRD, SEM, BET, XRF	Batch (10 g L^{-1}, 40–90 mg L^{-1}, 0–1440 min, 100 rpm, 25±2 °C, pH: 2.5, 4.5, 7)	Koble–Corrigan	Pseudo-second-order	Arabyarmohammadi et al. (2014)
	Clay tile	0.045–0.15, 2–4.760 mm, 0.1717 $m^2\,g^{-1}$ (0.595–1.190 mm)	1.76	XRD, SEM, BET, XRF	Batch (10 g L^{-1}, 40–90 mg L^{-1}, 0–1440 min, 100 rpm, 25±2 °C, pH: 2.5, 4.5, 7)	Koble–Corrigan	Elovich	Arabyarmohammadi et al. (2014)
Organic materials								
Cr(VI)-based ions	Cork waste	0.16–2, 0.08–0.16, <0.08 mm, 2.1095, 2.8545, 3.0245 $m^2\,g^{-1}$, 0.484, 0.656, 0.695 $cm^3\,g^{-1}$	N/A	FTIR, BET	Batch (1 g L^{-1}, 0.5–500 mg L^{-1}, pH: 1–5, 1–240 min)	BET	Pseudo-second-order	Sfaksi et al. (2014)
Cr(III) ions	Meranti Sawdust	0.1–0.15 mm, 25.34 nm, 0.62 $m^2\,g^{-1}$	37.878	SEM/EDX, FTIR, BET	Batch (20–100 g L^{-1}, 1–200 mg L^{-1}, pH: 1–8, 1–180 min, 100 rpm, 15–45 °C)	Langmuir and Dubinin–Radushkevich	Pseudo-second-order	Rafatullah et al. (2009)
Cu(II) ions	Meranti Sawdust	0.1–0.15 mm, 25.34 nm, 0.62 $m^2\,g^{-1}$	32.051	SEM/EDX,FTIR, BET	Batch (20–100 g L^{-1}, 1–200 mg L^{-1}, pH: 1–8, 1–180 min, 100 rpm, 15–45 °C)	Langmuir and Dubinin–Radushkevich	Pseudo-second-order	Rafatullah et al. (2009)
	Cherry sawdust	<2.00 mm	2.16	FTIR	Batch (10 g L^{-1}, 10–150 mg L^{-1}, 1440 min, 22±2 °C)	Langmuir	N/A	Kovacova et al. (2020)
	Spruce sawdust	<2.00 mm	2.48	FTIR	Batch (10 g L^{-1}, 10–150 mg L^{-1}, 1440 min, 22±2 °C)	Freundlich	N/A	Kovacova et al. (2020)

Table 3 (continued)

Adsorbate (ionic species)	Adsorbent	Adsorbent properties (Surface area ($m^2\ g^{-1}$), average pore diameter (nm), particle size (mm), average pore volume ($cm^3\ g^{-1}$))	Adsorption capacity (mg/g)	Characterization method	Adsorption technique (Batch/Column) and conditions (Dosage (g/g L^{-1}), Concentration (mg L^{-1}), Temperature (°C), pH, Agitation speed (rpm), Contact time (min), Bed depth (cm), flowrate ($mL\ min^{-1}$))	Isotherm model which best explain the adsorption behaviour	Kinetic model which best explain the adsorption behaviour	References
Ni(II) ions	Meranti Sawdust	0.1–0.15 mm, 25.34 nm, 0.62 $m^2\ g^{-1}$	35.971	SEM/EDX, FTIR, BET	Batch (20–100 g L^{-1}, 1–200 mg L^{-1}, pH: 1–8, 1–180 min, 100 rpm, 15–45 °C)	Langmuir and Dubinin–Radushkevich	Pseudo-second-order	Rafatullah et al. (2009)
Pb(II) ions	Meranti Sawdust	0.1–0.15 mm, 0.62 $m^2\ g^{-1}$, 25.34 nm	34.246	SEM/EDX, FTIR, BET	Batch (20–100 g L^{-1}, 1–200 mg L^{-1}, pH: 1–8, 1–180 min, 100 rpm, 15–45 °C)	Langmuir and Dubinin–Radushkevich	Pseudo-second-order	Rafatullah et al. (2009)
Zn(II) ions	Cherry sawdust	<2.00 mm	1.46	FTIR	Batch (10 g L^{-1}, 10–150 mg L^{-1}, 1440 min, 22±2 °C)	Langmuir	N/A	Kovacova et al. (2020)
	Spruce sawdust	<2.00 mm	2.01	FTIR	-	Freundlich	N/A	Kovacova et al. (2020)

*N/A not available

as another factor. The adsorption behaviour of marble waste towards different metal ions can be better understood by performing adsorption experiments changing the metal ion type while keeping the other factors (contact time, initial metal ion concentration, adsorption dose, etc.) constant.

Brick

Clay-based masonry materials including bricks significantly contribute to the generation of construction and demolition debris generation (see Table 2). Research has been conducted to evaluate the adsorption potential of brick powder towards heavy metal ion removal. Bibi et al. used commercially available bricks as a water treatment matrix for the removal of arsenic. The collected bricks from a kiln were washed with distilled water, dried, and ground to obtain a fine powder. XRD diffractograms have indicated quartz as the major component of the brick powder. The adsorption behaviour was modelled by the Langmuir isotherm model with a maximum adsorption capacity of 0.04 mg g^{-1} (Bibi et al. 2015).

Arabyarmohammadi et al. examined the potential of hand-made bricks (H-bricks) and machine-made bricks (M-bricks) to sequester Zn(II) ions from aqueous solutions. Based on BET analyses, the M-bricks and H-bricks specific surface areas were 1.2655 and 0.3317 $m^2\ g^{-1}$. According to XRF analysis, main mineral constituents of both adsorbents were identified as SiO_2, CaO, Al_2O_3, Fe_2O_3, MgO, and K_2O. Removal capacities of 3.9 mg g^{-1} and 2.45 mg g^{-1} were observed for the M-bricks and H-bricks, respectively. The maximum removal capacities for an initial 40 mg L^{-1} Zn(II) ion concentration, 10 g L^{-1} adsorbent dosage, at pH 6–7 were 75 and 50% for the M-bricks and H-bricks, respectively (Arabyarmohammadi et al. 2014). M-brick has higher adsorption potential towards Zn(II) ions compared to H-bricks. According to the results, the M-bricks have higher surface area than H-bricks. The higher specific surface area provides more active sites leading to adsorption enhancement (Rong et al. 2017). Therefore, M-bricks may have shown a higher removal capacity due to the higher surface area of M-bricks.

Zhang et al. performed column adsorption studies to investigate the potential of crushed brick to remove Cu(II) ions. The adsorbent mainly consisted of CaO, SiO_2, MgO, Al_2O_3, and Fe_2O_3. The best removal efficiency was observed at 0.5 mg L^{-1} Cu(II) ion concentration, 20 cm bed height, and a 12 min residence time. Sorption capacity values of 0.088, 0.104, and 0.1696 mg g^{-1} were obtained at initial metal ion concentrations of 0.5, 1.0, and 2.0 mg L^{-1} (Zhang et al. 2019).

The potential of the crushed bricks for removing Hg(II) from aqueous solutions has also been analysed. The adsorbent was characterized by performing XRD analysis which indicated that the sample was mainly composed of quartz, dolomite ($CaMg(CO_3)$, and $CaCO_3$. Batch adsorption studies

were conducted with varying solution pH, sorbent dosage, and contact time to determine the adsorption capacity for Hg(II) ions. The results indicated that isotherm data followed the Langmuir equation, and the obtained maximum removal capacity was 87 mg g^{-1} (Labidi 2008).

Hai et al. studied crushed laterite block in the particle size fractions 0.105–2 mm and < 0.105 mm for adsorptive removal of Cd(II) ions. Laterite is mainly composed of iron oxides, aluminium, and silica, and the chemical composition varies based on the formation. This material is abundantly available in tropical countries (Abhilash et al. 2016). The adsorption process followed the Freundlich adsorption isotherm model in the studied initial metal ion concentration range (25–900 mg L^{-1}). A percentage removal of 76 ± 7.7% was obtained at the initial metal ion concentrations 25 and 50 mg L^{-1} for the particle size fraction < 0.105 mm (Hai et al. 2018).

The results of these studies indicate that powdered brick also has potential for the adsorptive removal of heavy metal ions. These adsorption experiments have also been carried out under a wide range of adsorption conditions (initial metal ion concentration 0.04–500 mg L^{-1}, shaking speed 100–3500 rpm, etc., see Table 3). Therefore, further studies can be carried out to identify which brick types are most suitable for heavy metal ion treatment by changing the metal ion and the brick type used as an adsorbent while keeping the other adsorption conditions constant.

Roofing and flooring tiles

Clay tiles have been used to adsorb Zn(II) ions using three different particle sizes (45–150 μm, 0.595–1.190 mm, and 2–4.760 mm) to perform batch experiments. The main component of the adsorbent was SiO$_2$ according to XRF analysis, and SEM analysis showed the presence of pores with different sizes and shapes, which is favourable for the adsorption process. According to BET analyses, the surface area of the adsorbent was found to be 0.1717 m^2 g^{-1}. The Elovich kinetic model and Koble–Corrigan isotherm model (See the introduction section for more details on these isotherm models) were found to be the best explanation for the experimental data and the measured maximum removal capacity is 1.76 mg g^{-1} (Arabyarmohammadi et al. 2014).

Jelić et al. (2017) studied roof tiles from building ruins to adsorb Sr(II), Co(II), and Ni(II) ions. The main mineral phases of roof tiles identified according to XRD analysis were SiO$_2$ and albite (NaAlSi$_3$O$_8$). Based on adsorption kinetic studies, Sr(II) and Co(II) ions adsorption followed the pseudo-second-order kinetic model and with Ni(II) ions following the pseudo-first-order kinetic model with respect to adsorption. Adsorption capacities of 5.87, 3.83, and 2.63 mg g^{-1} were observed for Ni(II), Co(II), and Sr(II) ions, respectively. The Freundlich isotherm model was a better fit to the observed adsorption behaviour of all three metal ions (Jelić et al. 2017). Based on their results, the adsorbent has higher adsorption potential towards Ni(II) ions compared to Co(II) and Sr(II) ions. The difference in adsorption capacity might be attributed to electronegativity. Pauling's electronegativity of Ni (1.91) is higher than Co (1.88) and Sr (0.95). Therefore, Ni(II) ions might have exhibited comparatively greater affinity towards binding sites on the adsorbent (Selim et al. 2019).

Ceramics

Aluminosilicate minerals such as clay and zeolites have been investigated as adsorbents due to their potential to adsorb ionic species from aqueous solutions (Jiang et al. 2010; Elboughdiri 2020). Ceramic materials are also aluminosilicates based and therefore can be investigated for immobilization of heavy metal ions (Keppert et al. 2018).

A silica-based ceramic having the major chemical constituents; SiO$_2$, Na$_2$O, Al$_2$O$_3$, CaO, and K$_2$O was investigated as a removal agent of Pb(II) and As(III)-based ions from contaminated solutions. Both Pb(II) and As(III)-based ionic species exhibited adsorption behaviours which followed pseudo-second-order kinetics. For As(III) removal, there was a greater adherence in terms of the adsorption to the Freundlich isotherm model, whereas, for Pb(II) ions, the Langmuir isotherm model showed a better fit to adsorption data. The maximum adsorption capacity was reported to be 2.7 mg g^{-1} and 1.789 mg g^{-1} for Pb(II) and As(III)-based ions, respectively (Salim and Munekage 2009a, b).

Wood waste

Timber is one of the main contributors of CDW generation in some countries such as New Zealand and Norway (Table 2). The wood waste mainly consists of untreated and treated wood, waste wood mixed with virgin wood, sawdust, shavings, and off-cuts (Grace et al. 2016). Hardwood, softwood, and engineered wood are also used in construction projects and are common waste materials. The common hardwood species that are used for construction purposes include walnut, maple, oak, birch, and cherry. Spruce, pine, cedar, redwood, and fir are some of the frequently used softwood species in the construction sector. Engineered wood is thermally or chemically treated wood and the most popular examples are plywood, MDF (medium density fibreboard), composite board, and CLT (cross-laminated board) (Copeland 2020).

Many studies have been performed to investigate the capacity of timber waste to bind heavy metal ions. Wood is essentially composed of lignin, cellulose, and hemicellulose. However, the composition can vary based on the source (Ramage et al. 2017).

Meranti tree is a common tree found in tropical countries such as Indonesia and Malaysia and widely used in internal applications such as cabinetry, furniture, etc. Meranti wood sawdust, which mainly consists of cellulose, hemicellulose, lignin, and tannins, has been tested as an adsorbent for Cu(II), Cr(III), Ni(II), and Pb(II) ions. The BET surface area of the adsorbent was reported as 0.62 m^2 g^{-1}, and based on the SEM analysis, the adsorbent has a porous and irregular surface structure. FTIR analysis indicated the presence of functional groups such as phenolic OH, C=O, C=C, and C–O groups. The intensity and position of these peaks were found to be slightly affected after the adsorption process as elongation and shifting of these bands were observed after metal ion binding. Adsorption capacities of 37.878, 35.971, 34.246, and 32.051 mg g^{-1} were obtained for Cr(III), Ni(II), Pb(II), and Cu(II) ions, respectively, and the Langmuir isotherm model fitted well to the experimental data obtained (Rafatullah et al. 2009).

Researchers have also investigated the use of spruce and cherry sawdust for removal of Cu(II) and Zn(II) ions. Their results indicated that cherry sawdust showed maximum adsorption capacities of 1.46 and 2.16 mg g^{-1}, while spruce sawdust showed maximum adsorption capacities of 2.01, and 2.48 mg g^{-1} towards Zn(II) and Cu(II) ions, respectively (Kovacova et al. 2020). An adsorption preference can be observed for the Cu(II) ion adsorption compared to the Zn(II) ions for both adsorbents which is due to the higher electronegativity of Cu (1.90) compared to Zn (1.65) and the smaller hydrated radius of the Cu(II) ion (0.419 nm) compared to the Zn(II) ion (0.430 nm) (de Carvalho Izidoro et al. 2012; Chen et al. 2018). Metal ions with a smaller hydrated radius can easily enter the pores on the adsorbent to become adsorbed (de Carvalho Izidoro et al. 2012).

Sfaksi et al. tested waste cork powder obtained from cork board manufacturing factories for Cr(VI)-based ion adsorption and observed about 97% removal from solutions in the pH range 2–3. The adsorbent was characterized by performing FTIR and BET analysis which indicated the presence of macropores and functional groups such as C–O, O–H, and C=O on the adsorbent surface that favour metal ion binding. Their results further indicated that the adsorption process is highly influenced by parameters such as contact time, metal ion concentration, pH, and particle size (Sfaksi et al. 2014).

When comparing the adsorption capacities, Meranti sawdust seems to have a higher adsorption potential when compared with the spruce and cherry sawdust. Comparatively, the adsorption experiments of Meranti sawdust have been conducted under higher pH and temperature conditions (see Table 3). Lesser removal of metal ions occurs at lower pH values due to the competition between the H$^+$ ions and the metal ions for binding to the active sites on the adsorbent surface (Deng et al. 2007). The experiments of spruce and cherry sawdust have been conducted under a lower adsorbent dosage level compared to Meranti sawdust. More binding sites on the adsorbent is available for binding of metal ions at higher adsorbent dosages which favours the adsorption process (Jayarama et al. 2009). The adsorption capacities of these adsorbents can be better compared by performing adsorption experiments under the same adsorption conditions.

Development of modified adsorbents from CDW for water treatment

Previous discussion has centred on unmodified CDW and its application as a matrix for heavy metal removal. However, a number of modification methods have been applied to CDW which involve chemical modification, biochar production, and activated carbon production in order to investigate whether the adsorption capacity of the CDW adsorbents can be enhanced thorough these modifications. Table 4 summarizes the findings of the studies which used modified CDW-derived adsorbents for heavy metal treatment.

Chemical modification methods applied to CDW

Chemical modification refers to techniques that alter the surface properties and structure of adsorbents to improve the adsorption potential of these materials (Abegunde et al. 2020). Literature reports indicate that numerous chemical modification methods have been employed to improve the adsorption potential of adsorbents derived from CDW using acid, base, or mineral salts, etc., as the modification reagents.

Acid modifications improve the adsorption potential mainly by enhancing the porous nature of adsorbents, such as providing more surface area for adsorbate binding. A number of acids used for this purpose have been detailed in the literature and include hydrochloric acid (HCl), nitric acid (HNO$_3$), citric, malonic, and tartaric acid for adsorbent modification (Palma et al. 2003; Argun and Dursun 2006; Argun et al. 2007; Salazar-Rabago and Leyva-Ramos 2016). Oak sawdust modified by means of HCl (0.5–5 mol L^{-1}) treatment was applied as an adsorbent to remove Cu(II), Ni(II), and Cr(VI)-based ions. The HCl treatment was performed to enhance the proportion of active sites and to prevent elution of tannin compounds which might greatly increase the COD value of wastewater. The modified adsorbent was prepared by shaking 25 g of sawdust with 250 mL of HCl solution at 200 rpm for 4 h at 25 ℃. Maximum adsorption capacities of 3.22, 3.29, 1.70 mg g^{-1} were observed for Cu(II), Ni(II), and Cr(VI)-based ion adsorption, respectively, at 20 ℃ (Argun et al. 2007). According to the results, the adsorption capacity of Cr(VI)-based ions is comparatively low. The comparatively high adsorption capacity of Cu(II) and Ni(II) ions over Cr(VI) ions may have resulted from the smaller hydrated radii value of Cu(II) and Ni(II) ions which makes those ions

more accessible to the adsorbent pores (hydrated radii of Cu(II), Ni(II), and Cr(VI) are 0.419, 0.404, and 0.461 nm, respectively) (Chen et al. 2018; Obayomi et al. 2020).

A similar study was performed for Pb(II) ions removal using *Pinus durangensis* sawdust modified with citric, malonic, and tartaric acids at 0.5, 1, and 2 M concentrations. The SEM analysis of raw sawdust and modified sawdust indicated that the modification process enhanced the pores and channel-like structures on the surface. Moreover, FTIR analysis indicated that the modifications increased carboxylic group concentration in the adsorbents compared to the raw material. The authors of the study suggested that the COOH groups of the acids reacted with the O–H groups on the adsorbent surface via esterification reactions. The highest adsorption potential was displayed by sawdust modified with 1 M citric acid which was reported to be 304 mg g^{-1}, whereas natural sawdust showed an adsorption capacity of 18.9 mg g^{-1} (Salazar-Rabago and Leyva-Ramos 2016).

Comparatively, citric acid treatment seems to be very effective at improving the adsorption capacity of adsorbents derived from wood waste. Therefore, further analysis should be directed to this research area to explore its potential. On the other hand, some studies report that acid treatment decreased the adsorption potential of the adsorbents. For instance, cedar sawdust and crushed brick modified with H_2SO_4 and H_3PO_4 were inefficient and the sorption potential decreased for Cu(II) ions (Djeribi and Hamdaoui 2008). A similar observation was made by Argun and Dursun who investigated the adsorption potential of pine bark modified with HCl, HNO_3, and H_2SO_4 for Cd(II) and Pb(II) ion removal. They suggested that even though acid modifications improved the porosity of the adsorbent, the positively charged adsorbent surface prevented the enhancement of adsorption potential towards positively charged metal ions in these adsorbents (Argun and Dursun 2006).

Base modification can also enhance the surface area of the adsorbent and also affect the functional groups distribution on the adsorbent surface. NaOH, KOH, and Na_2CO_3 are some of the bases used as modification agents that have been reported in the literature (Šćiban et al. 2006; Djeribi and Hamdaoui 2008; Nagy et al. 2014; Kovacova et al. 2020).

A base-modified adsorbent (using 1 M NaOH and KOH) was synthesized using spruce sawdust for Cu(II) and Zn(II) ion sequestration. The treated material was washed with distilled water to remove the access base present on the adsorbent. The comparative analysis of FTIR spectra acquired of the unmodified and modified adsorbents indicated a significant intensification of the OH functional group in the modified adsorbent. The adsorption efficiency of KOH- and NaOH-modified spruce sawdust improved by 4.9 and 4.2 times, respectively, at 150 mg L^{-1} Zn(II) concentration compared to the unmodified adsorbent (Kovacova et al. 2020).

NaOH- and Na_2CO_3-pretreated fir sawdust has also been applied as an adsorbent for Cu(II) and Zn(II) ions from water. The modified adsorbent was prepared by treating one part of the sawdust with 15 parts of the modification agent using different concentrations. The modified adsorbent was washed with distilled water to remove excess base. The authors reported that base modifications improved the adsorption capacity of the adsorbent in comparison to raw sawdust from about 15 times enhancement for Zn(II) ions and 2.5 to 5 times for enhancement Cu(II) ions. Additionally, leaching of organic matters from modified adsorbent was about 23% less than unmodified adsorbent. However, the authors highlighted that the modification process leads to the generation of wastewater having high COD values and alkalinity (Šćiban et al. 2006). This negatively impacts efforts towards a circular economy.

Several other modification methods for CDW-derived adsorbents have also been reported in the literature; these are oxidative and mineral salt treatments.

Treatment with mineral salts (NaCl, KCl, Na_2HPO_4, and $NaHCO_3$) has been reported to be a very effective modification method for crushed brick to remove Cu(II) ions. The modification was performed by stirring 5 g of crushed brick with 0.5 L of 0.1 M solution of reagent at 300 rpm for 24 h. The sorption percentage of untreated adsorbent was 67.3% at 200 mg L^{-1} Cu(II) ion concentration and 5 g L^{-1} adsorbent dosage. Under the same conditions, adsorption percentages of 89.2%, 83.2%, 78.1%, and 73.6% were obtained for adsorbents modified with Na_2HPO_4, KCl, NaCl, and $NaHCO_3$, respectively (Djeribi and Hamdaoui 2008).

Nagy et al. investigated the use of oxidative treatment to improve the adsorption capacity of fir sawdust. Several reactions such as displacement of side chains and oxidative cleavage of the aromatic ring structures in the sawdust materials may occur during the oxidative treatment. These modifications can affect the adsorption capacity of the adsorbent. The modification was performed by treating 50 g of fir sawdust with 250 mL of 1 M H_2O_2 for 3 h. Maximum adsorption capacities calculated using the Langmuir model were 2.67 and 2.20 mg g^{-1} for treated and raw sawdust, respectively, for Cd(II) ion removal (Nagy et al. 2014).

Biochar and activated carbon production

Biochar is produced when organic biomass is pyrolysed with limited or no oxygen (Yuan et al. 2016). Biochar has been extensively investigated as a material for water treatment in recent years because it possesses high porosity, high surface area, and high adsorption efficiency. Several studies report the utilization of biochar generated from CDW waste materials such as wood chips, sawdust, and bark for water treatment (Jiang et al. 2016; Karunanayake et al. 2018; Poo et al. 2018; Wu et al. 2019). The adsorption potential of biochar

is dependent upon several factors including biomass source, preparation method, nature of pollutants, and reaction conditions (Tomczyk et al. 2020).

Several studies have investigated hardwood waste materials for biochar production (Jiang et al. 2016; Wu et al. 2019). The effectiveness of jarrah wood biochar to adsorb Cu(II) and Zn(II) ions has been investigated. Cation exchange capacity, surface alkalinity, and the negative surface charge of biochar have affected the adsorption capacity towards these divalent ions. Jarrah wood biochar has shown adsorption capacities for Cu(II) (4.39 mg g^{-1}) and Zn(II) (2.31 mg g^{-1}) ion treatment, and the adsorption process was found to follow the Langmuir isotherm model. The higher adsorption capacity of Cu(II) ions compared to the Zn(II) ions may have resulted due to the higher electronegativity of Cu (1.90) compared to the Zn (1.65) (Jiang et al. 2016). Wu et al. derived biochar (heating biomass in a muffle furnace at 600 °C for 4 h) using walnut, cherry wood, and bamboo wood chips for Cd(II) ion adsorption which had shown adsorption capacities of 18.06, 18.8, and 19.12 mg g^{-1}, respectively (Wu et al. 2019).

Softwood waste materials have also been investigated for biochar production. Pine wood sawdust-derived biochar has been tested as an adsorbent for heavy metal ion treatment. The results showed that biochar prepared at 700 °C removed 81% and 46% of Cu(II) and Cd(II) ions, respectively, from solution when using a dosage of 50 g L^{-1} biochar and an initial metal ion concentration of 500 mg L^{-1} (Poo et al. 2018). The prepared biochar has shown much higher affinity towards Cu(II) ions compared to Cd(II) ions. The higher electronegativity of Cu (1.90) compared Cd (1.69) can be suggested as one of the factors which may have led to the higher adsorption capacity towards Cu(II) ions (Selim et al. 2019).

Some researchers have employed modifications to biochar. For instance, Karunanayake et al. investigated the use of Douglas fir waste wood to produce Fe_3O_4 magnetized biochar for the removal of Cd(II) and Pb(II) ions. The biochar was produced by pyrolysing waste wood at 900–1000 °C for 1–10 s and Fe_3O_4 was induced to deposit by precipitation on the biochar by treating an aqueous solution of Fe(II)/Fe(III) with NaOH. Magnetic biochar can be easily removed from water after treatment of contaminants using a magnet, thus avoiding time-consuming steps like filtration and centrifugation. Maximum adsorption capacities of 27 and 11 mg g^{-1} were observed for magnetic biochar, whereas 40 and 16 mg g^{-1} were observed for raw fir biochar for Pb(II) and Cd(II) ions, respectively (Karunanayake et al. 2018). The higher adsorption capacity towards Pb(II) ions may have occurred due to the higher electronegativity of Pb (2.33) compared to Cd (1.69).

Activated carbon is a material with high internal surface area and porosity and commercially the most widely applied

of adsorbents for water treatment (Ioannidou and Zabaniotou 2007). Materials with high carbon content and low inorganic content can be used as raw materials for activated carbon generation (Tsai et al. 1997). Activated carbon production involves two steps: biochar production by pyrolysis of biomass and activation by modification of adsorbent. The activation of the carbonized material is achieved by physical or chemical activation (Gęca et al. 2022). Literature reports utilization of CDW such as wood chips and sawdust for activated carbon production (Tuomikoski et al. 2021).

The physical activation process utilizes oxidizing agents such as steam, CO_2, air, or mixtures of these materials. For instance, Tuomikoski et al. prepared activated carbon from spruce sawdust for the Zn(II), Co(II), and Ni(II) ion treatment. In their work, the sawdust was carbonized at 800 °C in a reactor followed by activation with water steam (120 g h^{-1} at 140 °C) for 120 min at 800 °C. The resultant adsorbent material had a considerably higher surface area (1010 m^2 g^{-1}) compared to that of activated carbon synthesized via other means in related studies. The highest maximum adsorption capacity was observed for Zn(II) ion removal experiments (23.413 mg g^{-1}), while for Co(II) and Ni(II) ions, the maximum adsorption capacities were comparatively low (5.371 and 8.580 mg g^{-1}, respectively). According to the results, the adsorbent had shown better adsorption potential towards Zn(II) ions compared to Co(II) and Ni(II) ions. The adsorption behaviour of Zn(II) ions is different from that of Ni(II) and Co(II) ions as Zn(II) adsorption follows pseudo-second-order adsorption kinetics while the Co(II) and Ni(II) ion adsorption was explained better by the Elovich kinetic model. The different metal ion adsorption behaviour on this adsorbent can be suggested as one of the factors which led to increased adsorption capacity towards Zn(II) ions (Tuomikoski et al. 2021).

The activation via chemical treatments of activated carbon has been achieved using agents such as acids and bases. Gao et al. prepared activated carbon from pine wood sawdust for Cu(II) ion adsorption. Phosphoric acid (85% wt) was used to further activate the carbonized material. According to BET analysis, the surface area of the activated carbon significantly improved with acid treatment (Gao et al. 2018). In a similar study, biochar derived from pine sawdust was modified by treating with 47.5% wt. H_3PO_4 solution at room temperature for 24 h. The surface area analysis indicated that the acid-modified biochar had a higher surface area compared to the unmodified biochar prepared under the same conditions. The modified biochar showed 4–13 times and 12–44 times higher adsorption capacity towards Cd(II) and Cu(II) ions, respectively, compared to the unmodified adsorbent (Peng et al. 2017).

NaOH-activated cedar wood has been applied to achieve Pb(II) ion removal. The wood samples were carbonized at 500 °C for 2 h under a nitrogen atmosphere. For activation,

Table 4 Application of modified construction and demolition waste in heavy metal ion removal from aqueous solutions

Adsorbate (ionic species)	Adsorbent	Adsorbent properties (Surface area (m² g⁻¹), average pore diameter (nm), particle size (mm), average pore volume (cm³ g⁻¹), BC/AC production temperature (°C))	Adsorption capacity (mg g⁻¹)	Characterization method	Adsorption technique (Batch/Column) and conditions (Dosage (g L⁻¹), Concentration (mg L⁻¹), Temperature (°C), pH, Agitation speed (rpm), Contact time (min))	Isotherm model which best explain the adsorption behaviour	Kinetic model which best explain the adsorption behaviour	References
Cd(II) ions	Magnetized Douglas fir biochar	459.0 m² g⁻¹, 0.158 cm³ g⁻¹, 0.1–0.6 mm, 900–1000 °C	11	SEM-EDX, TEM-EDS, BET, XRD	Batch (2, 0.4 g L⁻¹, 10–250 mg L⁻¹, 25–45 °C, 0–1440 min, pH: 2–7)	Langmuir and Freundlich	N/A	Karunanayake et al. (2018)
	KOH-activated Douglas fir biochar	0.1–0.5 mm, 1050 m² g⁻¹, 0.672 cm³ g⁻¹, 2.56 nm, 900–1000 °C	29	SEM-EDX, TEM-EDS, XPS, TGA, BET	Batch (1 g L⁻¹, 25–1000 mg L⁻¹, 0–1440 min, pH: 2–10)	Langmuir	Pseudo-second-order	Herath et al. (2021)
	Acid-modified pine sawdust biochar	<0.2 mm, 599–900 m² g⁻¹, 200–650 °C	N/A	FTIR, XPS, BET	Batch (0.25 g L⁻¹, 1–10 mg L⁻¹, 7200 min, pH:5 ± 0.1, 100 rpm)	Freundlich	N/A	Peng et al. (2017)
	Walnut biochar Cherry biochar Bamboo biochar	600 °C 600 °C 600 °C	18.06 18.8 19.12	FTIR, SEM	Batch (0.2–7 g L⁻¹, 5–60 mg L⁻¹, 120 rpm, 25 °C, 5–120 min, pH: 2–9)	Langmuir	Pseudo-second-order	Wu et al. (2019)
	Pine sawdust biochar	700 °C, 419.1 m² g⁻¹, 0.18–1.7 mm	5.04	SEM-EDX, BET, FTIR	Batch (50 g L⁻¹, 500 mg L⁻¹, 30 min)	N/A	N/A	Poo et al. (2018)
	H₂O₂ treated fir sawdust	0.4–0.6 mm	2.67	FTIR	Batch (50 g L⁻¹, 50–365 mg L⁻¹, 700 rpm, 23 °C, 0–240 min)	Langmuir	Pseudo-second-order	Nagy et al. (2014)
Co(II) ions	Spruce sawdust activated carbon	1.4–2 mm, 1010 m² g⁻¹, 2.8 nm, 800 °C	5.371	BET	Batch (0.5–10 g L⁻¹, 30–900 mg L⁻¹, 1–1440 min, pH: 2–7)	Freundlich	Elovich	Tuomikoski et al. (2021)

Table 4 (continued)

Adsorbate (ionic species)	Adsorbent	Adsorbent properties (Surface area ($m^2 g^{-1}$), average pore diameter (nm), particle size (mm), average pore volume ($cm^3 g^{-1}$), BC/AC production temperature (°C))	Adsorption capacity (mg g^{-1})	Characterization method	Adsorption technique (Batch/Column) and conditions (Dosage (g L^{-1}), Concentration (mg L^{-1}), Temperature (°C), pH, Agitation speed (rpm), Contact time (min))	Isotherm model which best explain the adsorption behaviour	Kinetic model which best explain the adsorption behaviour	References
Cr(VI)-based ions	KOH-activated Douglas fir biochar	0.1–0.5 mm, 1050 $m^2 g^{-1}$, 0.672 $cm^3 g^{-1}$, 2.56 nm, 900–1000 °C	127.2	SEM–EDX, TEM–EDS, XPS, TGA, BET	Batch (1 g L^{-1}, 25 –1000 mg L^{-1}, 0–1440 min, pH: 2–10)	Langmuir	Pseudo-second-order	Herath et al. (2021)
	HCl treated oak sawdust	<0.25 mm	1.70	N/A	Batch (5–80 g L^{-1}: 0.1–100 mg L^{-1}, pH: 2–9, 100–450 rpm, 20–40 °C, 0–720 min)	Langmuir and Dubinin-Radushkevich	Pseudo-second-order	Argun et al. (2007)
Cu(II) ions	H_3PO_4-activated pinewood sawdust	0.56–0.9 mm, 500–800 °C, 1537.5–1750.7 $m^2 g^{-1}$, 1.8920-4.1145 nm	N/A	BET, SEM, FTIR	Batch (2 g L^{-1}, 25–200 mg L^{-1}, 0–90 min, pH: 2–6, 300 rpm, 25 °C)	N/A	Pseudo-second-order	Gao et al. (2018)
	Ultrasound pre-treated softwood biochar	503.60 $m^2 g^{-1}$, 800 °C	19.99	SEM–EDX, FTIR, BET	Batch (5 g L^{-1}, 10–100 mg L^{-1}, 25–60 °C, 0–60 min, 150 rpm)	Freundlich	Pseudo-second-order	Peter et al. (2021)
	Acid-modified pine sawdust biochar	<0.2 mm, 599–900 $m^2 g^{-1}$, 200–650 °C	N/A	FTIR, XPS, BET	Batch (0.25 g L^{-1}, 1–10 mg L^{-1}, 7200 min, pH:5±0.1, 100 rpm)	Freundlich	N/A	Peng et al. (2017)
	Jarrah wood biochar	700 °C, <1 mm	4.39	N/A	Batch (25 g L^{-1}, 120 rpm, 25 °C, 1440 min, pH: 2–6)	Langmuir	N/A	Jiang et al. (2016)
	NaOH-pretreated fir sawdust	0.5–1.0 mm	12.71	N/A	Batch(5 g L^{-1}, pH 4, 180 min)	Langmuir	N/A	Šćiban et al. (2006)

Table 4 (continued)

Adsorbate (ionic species)	Adsorbent	Adsorbent properties (Surface area ($m^2\,g^{-1}$), average pore diameter (nm), particle size (mm), average pore volume ($cm^3\,g^{-1}$), BC/AC production temperature (°C))	Adsorption capacity (mg g^{-1})	Characterization method	Adsorption technique (Batch/Column) and conditions (Dosage (g L^{-1}), Concentration (mg L^{-1}), Temperature (°C), pH, Agitation speed (rpm), Contact time (min))	Isotherm model which best explain the adsorption behaviour	Kinetic model which best explain the adsorption behaviour	References
	NaOH treated spruce sawdust	<2 mm	7.53±0.98	FTIR	Batch (10 g L^{-1}, 10–150 mg L^{-1}, 1440 min, 22±2 °C	N/A	N/A	Kovacova et al. (2020)
	HCl treated oak sawdust	<0.25 mm	3.22	N/A	Batch (5–80 g L^{-1}: 0.1–100 mg L^{-1}, pH: 2–9, 100–450 rpm, 20–40 °C, 0–720 min)	Langmuir and Dubinin-Radushkevich	Pseudo-second-order	Argun et al. (2007)
	Pine sawdust biochar	700 °C, 419.1 $m^2\,g^{-1}$, 0.18–1.7 mm	8.86	SEM–EDX, BET, FTIR	Batch (50 g L^{-1}, 500 mg L^{-1}, 30 min)	N/A	N/A	Poo et al. (2018)
Ni(II) ions	Spruce sawdust activated carbon	1.4–2 mm, 1010 $m^2\,g^{-1}$, 2.8 nm, 800 °C	8.580	BET	Batch (0.5–10 g L^{-1}, 30–900 mg L^{-1}, 1–1440 min, pH: 2–7)	Freundlich	Elovich	Tuomikoski et al. (2021)
	HCl treated oak sawdust	<0.25 mm	3.29	N/A	Batch (5–80 g L^{-1}: 0.1–100 mg L^{-1}, pH: 2–9, 100–450 rpm, 20–40 °C, 0–720 min)	Langmuir and Dubinin-Radushkevich	Pseudo-second-order	Argun et al. (2007)

Table 4 (continued)

Adsorbate (ionic species)	Adsorbent	Adsorbent properties (Surface area (m² g⁻¹), average pore diameter (nm), particle size (mm), average pore volume (cm³ g⁻¹), BC/AC production temperature (°C))	Adsorption capacity (mg g⁻¹)	Characterization method	Adsorption technique (Batch/Column) and conditions (Dosage (g L⁻¹), Concentration (mg L⁻¹), Temperature (°C), pH, Agitation speed (rpm), Contact time (min))	Isotherm model which best explain the adsorption behaviour	Kinetic model which best explain the adsorption behaviour	References
Pb(II) ions	Magnetized Douglas fir biochar	459.0 m² g⁻¹, 0.158 cm³ g⁻¹, 0.1–0.6 mm, 900–1000 °C	27	SEM–EDX, TEM-EDS, BET, XRD	Batch (2, 0.4 g L⁻¹, 10–250 mg L⁻¹, 25–45 °C, 0–1440 min, pH: 2–7)	Langmuir and Freundlich	N/A	Karunanayake et al. (2018)
	KOH-activated Douglas fir biochar	0.1–0.5 mm, 1050 m² g⁻¹, 0.672 cm³ g⁻¹, 2.56 nm, 900–1000 °C	140	SEM–EDX, TEM-EDS, XPS, TGA, BET	Batch (1 g L⁻¹, 25–1000 mg L⁻¹, 0–1440 min, pH: 2–10)	Langmuir	Pseudo-second-order	Herath et al. (2021)
	Citric acid-modified *Pinus durangensis* sawdust	0.16 mm, <0.4 m² g⁻¹	304	SEM, FTIR, BET	Batch (1.11–2.22 g L⁻¹, pH: 2–5, 300 rpm, 25 °C)	Redlich–Peterson	N/A	Salazar-Rabago and Leyva-Ramos (2016)
	NaOH-activated cedar wood	<0.1 mm, 2125 m² g⁻¹, 1.71 nm, 0.91 cm³ g⁻¹, 500 °C	971.9	FTIR, BET, SEM	Batch (0.25–1 g L⁻¹, pH 2–5, 0–120 min, 20–50 °C, 25–300 mg L⁻¹)	Freundlich	Pseudo-second-order	Rahmatnia et al. (2021)
Zn(II) ions	Spruce sawdust activated carbon	1.4–2 mm, 1010 m² g⁻¹, 2.8 nm, 800 °C	23.413	BET	Batch (0.5–10 g L⁻¹, 30–900 mg L⁻¹, 1–1440 min, pH: 2–7)	Freundlich	Pseudo-second-order	Tuomikoski et al. (2021)
	NaOH-pretreated fir sawdust	0.5–1.0 mm, 3.85 m² g⁻¹	13.4	BET	Batch(5 g L⁻¹, pH 6, 180 min)	Langmuir	N/A	Ščiban et al. (2006)
	Jarrah wood biochar	700 °C, <1 mm	2.31	N/A	Batch (Dose: 25 g L⁻¹, 120 rpm, 25 °C, 1440 min, pH: 2–6)	Langmuir	N/A	Jiang et al. (2016)
	KOH treated spruce sawdust	<2 mm	9.26 ± 1.68	FTIR	Batch (10 g L⁻¹, 10–150 mg L⁻¹, 1440 min, 22 ± 2 °C)	N/A	N/A	Kovacova et al. (2020)

*BC biochar, AC activated carbon

the obtained materials were stirred for 2 h using a biomass/NaOH ratio of 1:2. The prepared adsorbent was characterized by FTIR, SEM, and BET analysis. SEM analysis revealed that the adsorbent possessed a highly porous surface structure and FTIR spectra demonstrated the presence of functional groups such as C=O and C=C which have the potential to bind heavy metal ions (Rahmatnia et al. 2021). Herath et al. investigated KOH-activated Douglas fir biochar for Pb(II), Cr(VI), and Cd(II) ion adsorption. Douglas fir wood chips-derived biochar was stirred with KOH (4.00 g dissolved in 20 mL of distilled water) for 1 h. Based on the BET analysis, the surface area and the pore volume of the adsorbent were significantly increased after base treatment. Maximum adsorption capacities of 29, 140, and 127.2 mg g^{-1} were obtained at 318 K for treated adsorbent, whereas untreated adsorbent showed maximum adsorption capacities of 18, 84.1, and 33.5 mg g^{-1} for Cd(II), Pb(II) and Cr(VI)-based ions, respectively (Herath et al. 2021). Peter et al. have studied base activated (using NaOH) biochar derived from ultrasound pretreated (170 kHz, 1000 W, 80 ℃, 2 h) softwood woodchips for Cu(II) ion removal from water. According to SEM analyses, the ultrasound pretreatment significantly enhanced the microchannels on the adsorbent surface which improved the adsorption process. EDX mapping results showed the presence of sodium ions on the adsorbent surface after base modification. This observation has been stated as a good indication that the adsorbents can provide cation exchange ability which is an important metal ion removal mechanism. Furthermore, their results indicated that the adsorbent exhibited an equilibrium adsorption capacity of 19.99 mg g^{-1} which was about 22 times higher than the value for the corresponding non-activated adsorbent (Peter et al. 2021).

Based on the results, NaOH-activated cedar wood, Citric acid-modified *Pinus durangensis* sawdust, and KOH-activated Douglas fir biochar showed higher adsorption capacity towards heavy metal ion adsorption (specifically for Pb(II) and Cr(VI)-based ions) compared to the other adsorbents. However, the adsorption experiments were performed under different adsorption conditions (see Table 4). For instance, adsorption studies of KOH-activated Douglas fir biochar had been performed under higher initial metal ion concentration conditions (25–1000 mg L^{-1}) compared to other adsorbents (magnetized fir biochar; 10–250 mg L^{-1}, walnut biochar 5–60 mg L^{-1}). The adsorption capacities of these adsorbents can be better compared if the adsorption experiments were performed under the same adsorption conditions.

Heavy metal ion removal mechanisms involved with CDW-derived adsorbents

Heavy metal ion removal mechanisms are influenced by physical and chemical interactions between the adsorbent and adsorbate and the physical form of the adsorbent (Elwakeel et al. 2020). In literature, the heavy metal ion removal mechanism is proposed on the basis of the micro-structure analysis and adsorption kinetics and isothermal results. These mechanisms can occur in many complex forms, and several mechanisms can take place simultaneously (Putra et al. 2014). The most common heavy metal ion removal mechanisms of CDW-derived adsorbents include ion exchange, micro-precipitation, chemisorption mechanisms such as complexation, and physisorption mechanisms such as electrostatic interaction all of which are illustrated in Fig. 2 (Ray et al. 2020).

Ion exchange

Ion exchange involves the replacement of heavy metal ions in the solution with similarly charged ions attached to the adsorbent (Elwakeel et al. 2020). Ions present on the adsorbent surface such as Ca^{2+}, Na^+, and K^+ ions can participate in the adsorption process of heavy metal ions. For instance, Ca^{2+} ion exchange on the hydrated adsorbent surface has been identified as the main adsorption mechanism for autoclave aerated concrete (AAC) fines (Kumara et al. 2019). Ion exchange mechanisms have also been observed with adsorbents including *Pinus durangensis* sawdust (Salazar-Rabago and Leyva-Ramos 2016), marble waste (Ghazy and Gad 2014), NaOH- and Na_2CO_3-pretreated fir sawdust (Šćiban et al. 2006), and spruce sawdust and cherry sawdust (Kovacova et al. 2020). The functional groups on the adsorbent surface such as COOH and phenolic OH groups participate in the metal ion binding by exchanging H^+ ions with the metal ions in adsorbents such as *Pinus durangensis* sawdust, spruce sawdust, and cherry sawdust (Salazar-Rabago and Leyva-Ramos 2016; Kovacova et al. 2020). Ion exchange mechanisms are involved in the metal ion adsorption process undergone by marble waste through the exchange of Ca^{2+} ions present in $CaCO_3$ which is a major constituent of marble waste with metal ions from solution (Ghazy and Gad 2014). NaOH- and Na_2CO_3-pretreated fir sawdust utilized ion exchange mechanism in the adsorption process by exchanging Na^+ ions with metal ions. This mechanism was confirmed by the release of Na^+ ions during the adsorption process (Šćiban et al. 2006).
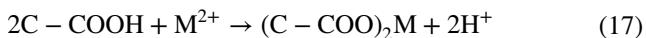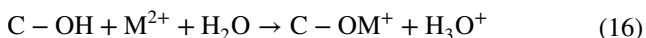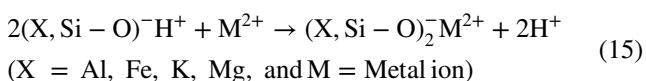
Complexation

Complexation involves the coordination of heavy metal ions with the functional groups on the adsorbents which can act as electron donors (Elwakeel et al. 2020). Complexation has been reported as a mechanism of metal ion adsorption for spruce and cherry sawdust (Kovacova et al. 2020), AAC fines (Kumara et al. 2019), and H_3PO_4-modified pine sawdust biochar (Peng et al. 2017). The involvement of complexation adsorption mechanisms in heavy metal ion binding on to AAC fines is explained by Eq. (15) (Kumara et al. 2019). The

Fig. 2 Heavy metal ion removal mechanisms of CDW-derived adsorbents. Based on the information of (Peng et al. 2017; Bartoli et al. 2020; Kovacova et al. 2020)
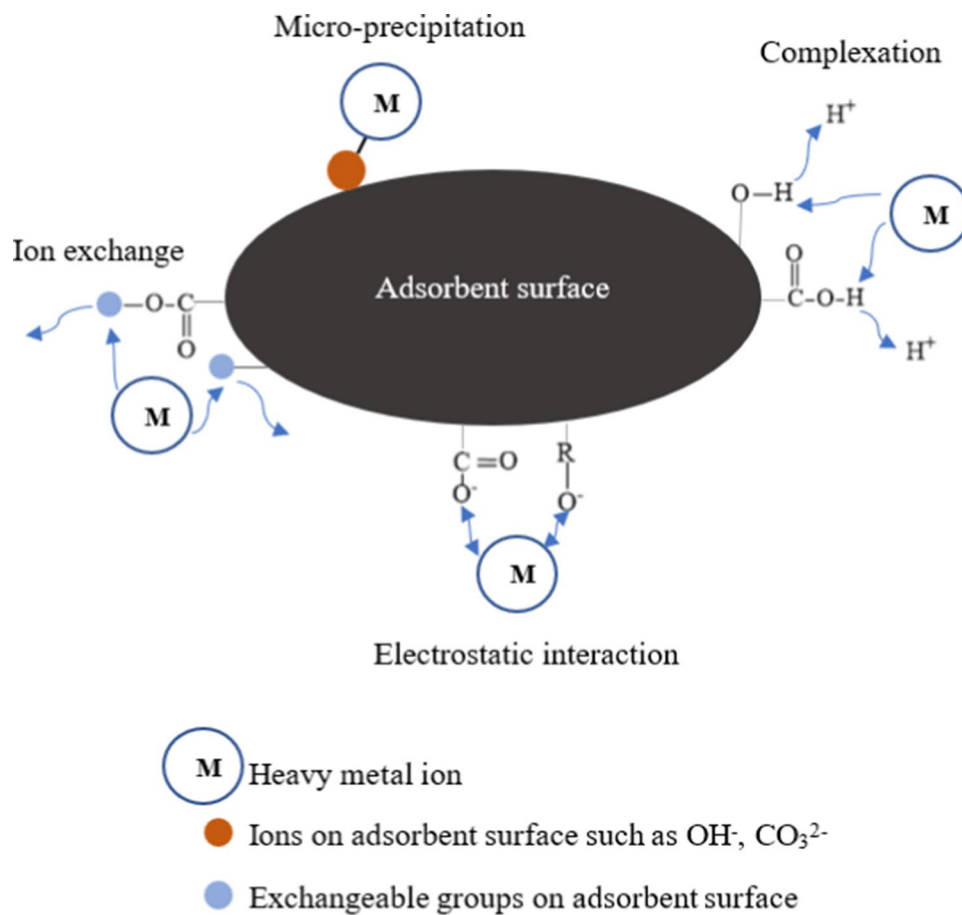
presence of functional groups such as –COOH/–OH groups on the surface of sawdust and biochar facilitate metal ion binding via the complexation mechanism (Peng et al. 2017; Kovacova et al. 2020). This adsorption mechanism is further explained in Eqs. (16) and (17) (Peng et al. 2017).

$$2(X, Si - O)^- H^+ + M^{2+} \rightarrow (X, Si - O)_2^- M^{2+} + 2H^+ \quad (15)$$
$$(X = Al, Fe, K, Mg, \text{ and } M = Metal\,ion)$$

$$C - OH + M^{2+} + H_2O \rightarrow C - OM^+ + H_3O^+ \quad (16)$$

$$2C - COOH + M^{2+} \rightarrow (C - COO)_2 M + 2H^+ \quad (17)$$

Micro-precipitation

Micro-precipitation is a process by which a substance is separated from a solution by forming a chemical precipitate as fine particles. For instance, the main heavy metal ion removal mechanism for dried concrete sludge was identified as metal hydroxide coprecipitation on the surface under high pH conditions (Yoo et al. 2018). Additionally, this mechanism has been suggested as a principal mechanism of metal ion

removal in materials such as crushed concrete fines (Coleman et al. 2005), autoclaved aerated concrete (Kumara et al. 2019), marble waste (Ghazy and Gad 2014), and NaOH- and Na₂CO₃-pretreated fir sawdust (Šćiban et al. 2006).

Electrostatic interaction

The electrostatic interactions between the heavy metal ions and the surface charges on the adsorbent represent another mechanism involved in heavy metal remediation (Qiu et al. 2021). The pH of the adsorption medium greatly affects the strength of the electrostatic interactions (Özdes et al. 2020). This type of adsorption behaviour has been observed with adsorbents such as acid-modified *Pinus durangensis* sawdust (Salazar-Rabago and Leyva-Ramos 2016) and H₂SO₄-modified oak wood sawdust (Özdes et al. 2020).

Comparison of adsorption performance exhibited by CDW materials

The results of the studies summarized in this article show that factors such as contact time, adsorbent dosage, initial metal ion concentration, shaking speed, pH of the medium,

Table 5 Batch adsorption results of biosorbents, geomaterials, and nanostructured materials for heavy metal treatment

Adsorbent	Adsorbate (ionic species)	Adsorption capacity (mg/g)	Adsorption conditions (Dosage (g L^{-1}), Concentration (mg L^{-1}), Temperature (℃), pH, Agitation speed (rpm), Contact time (min))	References
Biosorbents				
Sugarcane bagasse	Cu(II) ions	3.65	4 g L^{-1}, 10–200 mg L^{-1}, pH 2–6, 100 rpm, 90 min	Putra et al. (2014)
Aspergillus niger	Cd(II) ions	69.44	0.5–1 g L^{-1}, 20–100 mg L^{-1}, 220 rpm, 30 ℃, 0–35 min	Tsekova et al. (2010)
Lentinus edodes	Hg(II) ions	336.3 ± 3.7	1 g L^{-1}, 25–60 mg L^{-1}, pH 3–7, 400 rpm, 25 ℃	Bayramoğlu and Arıca (2008)
Pseudomonas aeruginosa	Ni(II) ions	70	1 g L^{-1}, 0–160 mg L^{-1}, 200 rpm, 0–60 min, 30 ± 2 ℃, pH 2–6	Gabr et al. (2008)
	Pb(II) ions	79		
Natural and industrial geomaterials				
Phosphatic clay	Pb(II) ions	37.2	30 ± 1 rpm, 0–200 mg L^{-1}, 25 ± 3 ℃, 8640 min	Singh et al. (2001)
	Cd(II) ions	24.5		
	Zn(II) ions	25.1		
Activated bentonite	Co(II) ions	7.3	2.5–40 g L^{-1}, 2–60 min, 25 ± 2 ℃, 20–250 mg L^{-1}, 200 rpm	Al-Shahrani (2014)
Modified clay	Ni(II) ions	80.9	10–200 mg L^{-1}, 1440 min, 20 ± 1 ℃	Vengris et al. (2001)
	Zn(II) ions	83.3		
	Cu(II) ions	63.2		
Nanostructured materials				
Multi-walled carbon nanotubes	Ni(II) ions	18.083	0.4 g L^{-1}, 10–200 mg L^{-1}, pH 2–7, 0–180 min	Kandah and Meunier (2007)
Single-walled carbon nanotubes	Zn(II) ions	43.66	0.5 g L^{-1}, 10–80 mg L^{-1}, 25 ℃, 180 rpm, 720 min, pH 1–12	Lu and Chiu (2006)
Multi-walled carbon nanotubes	Zn(II) ions	32.68		
Graphene nanosheets	Pb(II) ions	22.42	0.5 g L^{-1}, 5–80 mg L^{-1}, 30 ± 0.5 ℃, pH 2–8, 360 min	Huang et al. (2011)
Graphene	Sb(III)-based ions	10.92	0.4 g L^{-1}, 200 rpm, 30 ℃, 1–10 mg L^{-1}, pH 3–11, 30–240 min	Leng et al. (2012)

etc., greatly influence the adsorption performance of the adsorbent. Adsorption experiments of CDW-derived adsorbents have been performed under a wide range of adsorption conditions as summarized in Tables 3 and 4. As these experiments have been performed under various adsorption conditions, it is difficult to directly compare the adsorption performance of the adsorbents (De Gisi et al. 2016; Keppert et al. 2018). However, all the adsorbents discussed in this article have shown potential for heavy metal ion removal.

Under the same adsorption conditions, some CDW-derived adsorbents have shown higher adsorption potential towards a particular heavy metal ion compared to other heavy metal ions or vice versa. For instance, roof tiles have shown higher adsorption potential towards Ni(II) ions compared to Co(II) and Sr(II) ions (Jelić et al. 2017), and machine-made bricks have shown higher adsorption

potential towards Zn(II) ions compared to hand-made bricks (Arabyarmohammadi et al. 2014). Literature reports several factors which may cause this behaviour, such as pore size distribution of the adsorbent, size of the solvated metal ion, surface charge of adsorbent and adsorbate, and electronegativity of the metal ion (Liu et al. 2015; Baroud 2021). However, understanding the specific reasons for these behaviours still remains a scientific challenge and requires further investigations (Liu et al. 2015).

Table 5 summarizes the adsorption capacities of the most commonly studied adsorbents. Comparatively, inorganic CDW materials show similar potential for heavy metal ion treatment to the reported natural and industrial geomaterials. The organic CDW materials also show similar adsorption potential to the reported biosorbents and carbon-based nanomaterials (see Tables 3 and 4).
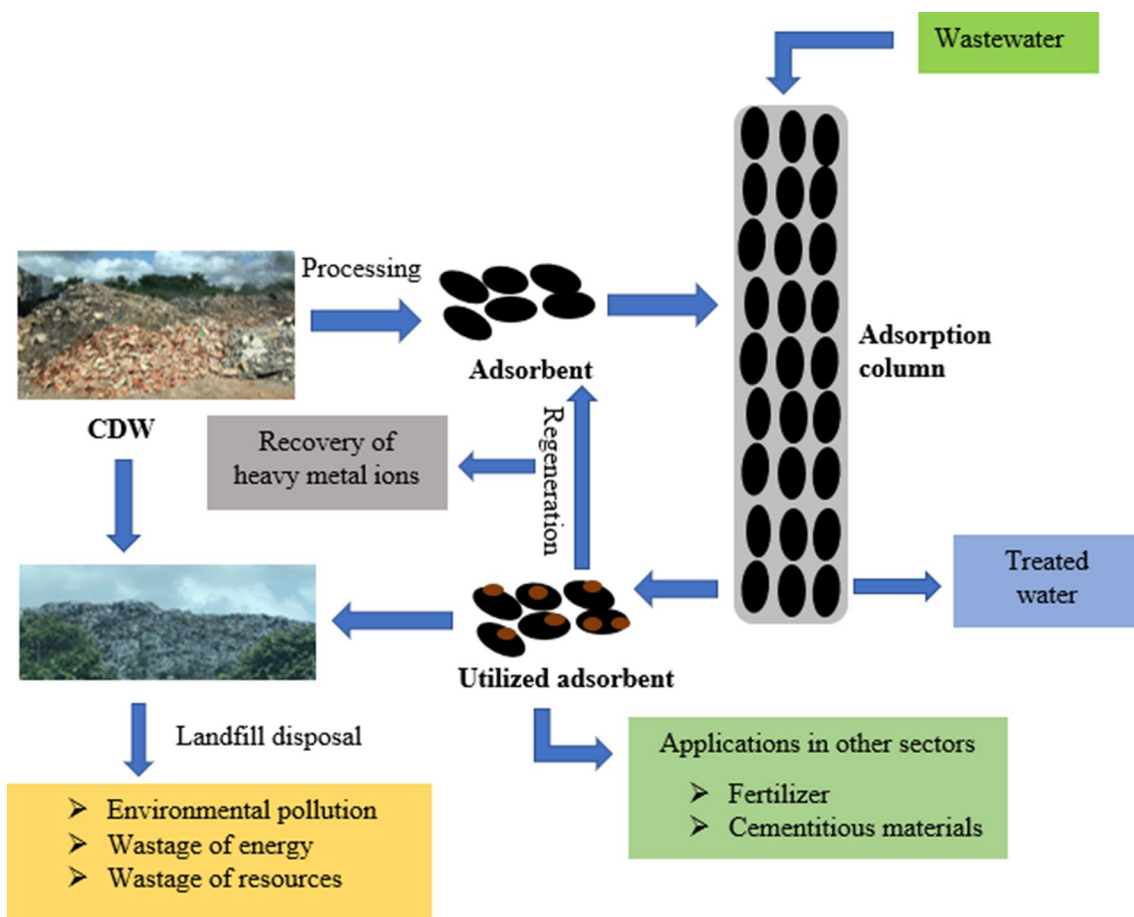
Fig. 3 Pathway of wastewater treatment by CDW and potential applications of utilized adsorbents

Applications of CDW-derived adsorbents containing adsorbed heavy metal ions (post adsorption)

Disposal of heavy metal treated adsorbents in landfills can be environmentally hazardous due to the existence of the heavy metals within the treated adsorbents and the risk of leaching from these adsorbents over time. Therefore, to prevent any further environmental pollution and to achieve circular economy goals, researchers have investigated potential regeneration and reutilization strategies for spent CDW adsorbents (Fig. 3).

Regeneration of treated adsorbents via desorption

The reuse of the heavy metal treated adsorbents is very important as it affects the economic success for the adsorbents and contributes to the idea of a circular economy. For instance, after the treatment of large volumes of wastewater, the treated adsorbents can be regenerated. The concentrated solution of heavy metal ions obtained after regeneration can be used to recover the metal ions via precipitation,

electrolytic means, etc., or reuse for industrial applications. Literature reports several desorption solvents which can be used to regenerate the heavy metal-laden adsorbents such as distilled water, acids (such as H_2SO_4, HCl), and bases (such as NaOH) (Coleman et al. 2005; Karunanayake et al. 2018; Ali and Abd Ali 2020; Herath et al. 2021).

Distilled water was investigated as a regeneration solvent to treat the portion of metal ions bound to the concrete fines without precipitation. These experiments were performed by treating the utilized adsorbent with water at 0.1 g cm^{-3} solid: solution ratio for 24 h. However, the authors reported that only a very small percentage of the adsorbed ions were readily soluble when using just water as a desorption solvent (Cu(II), 1.9%; Zn(II), 0.9% and Pb(II), 0.2%) (Coleman et al. 2005). A similar experiment was performed by Ali et al. with heavy metal-laden crushed concrete demolition waste, and their results also indicated that a very small percentage of the bound metal ions was leached from the adsorbent (Pb(II), 0.004% and Ni(II), 0%) (Ali and Abd Ali 2020).

In contrast when acids are used for heavy metal ion desorption, there is a competition between metal ions and H$^+$ ions at low pH to bind to the active sites and these binding

sites hence tend to become protonated so causing metal ions to desorb from the adsorbent surface (Lata et al. 2015; Krishnamoorthy et al. 2019). Palma et al. performed desorption experiments for metal ion-laden modified pine bark by treating 100 mg of the adsorbent with 10 mL H_2SO_4 (1–5 M) for 1 h. Metal ions such as Cu(II) and Hg(II) were observed to be readily desorbed (47–50.5% and 18–62%, respectively), whereas metal ions such as Cd(II) and Pb(II) desorbed less readily (1.8–2.7% and 0.8–1.4%, respectively). Regeneration of KOH-activated Douglas fir biochar has been investigated using 0.1 M HCl with which almost all adsorbed Pb(II) ions were reported to be successfully desorbed from the biochar. However, the adsorption potential of the adsorbent significantly dropped from 100 mg g^{-1} in the first cycle to 52 mg g^{-1} and 49 mg g^{-1} in the second and third regeneration cycles, respectively. The authors suggest that this may have occurred due to some chemical changes on certain binding sites after the first regeneration cycle (Herath et al. 2021).

Regeneration of Fe_3O_4-magnetized biochar and raw Douglas fir biochar has also been investigated using a 0.1 M HCl solution. Desorption experiments were carried out by treating 0.25 g of the loaded adsorbent with a 50 mL of 0.1 M HCl for 10 min followed by stirring with 10 mL of water for 10 min. At the first regeneration cycle, 41% of the adsorbed Cd(II) and Pb(II) ions were desorbed from the raw biochar whereas 87% and > 75% of the Cd(II) and Pb(II) ions were desorbed from the magnetic biochar, respectively. The authors suggested that the amount of tightly held Cd(II) and Pb(II) ions on magnetic biochar is less than that on the raw biochar. The adsorption of Cd(II) and Pb(II) ions was reduced by a few per cent in the second and third regeneration cycles for both modified and unmodified biochar (Karunanayake et al. 2018).

Alkali solvents have also been investigated as desorbing agents. For instance, an experimental study investigated the use of 0.1 M NaOH to desorb Cr(VI)-based ions from raw Douglas fir biochar and KOH-activated Douglas fir biochar. They observed that the amount of metal ions desorbed was considerably lower compared to the amount adsorbed in each cycle. The authors suggested that strong chemisorption of metal ions occurs on the adsorbent surface which will discourage desorption. Adsorption of Cr(VI)-based ions was observed to drop off after the first regeneration cycle in this study as well (Herath et al. 2021).

Use of heavy metal-laden materials in other applications

The use of heavy metal-laden adsorbents for other applications has also been investigated by researchers as a way to minimize waste. Mosoarca et al. demonstrated the potential use of oak wood ash for the treatment of wastewater contaminated with Mn(II) ions. The used (heavy metal-laden) adsorbent received after the adsorption process had been tested as a soil amendment for *Hordeum vulgare* (a barley crop). The experiment was performed by using various wood ash/soil weight ratios from 1:25 to 1:100 along with a control sample without adding the wood ash. After 28 days from seed sowing, growth parameters such as germination percentage, the height of the plant, and relative growth rate were evaluated and demonstrated improvement compared to the control samples (germination rate; up to 10% higher, average length; 14–35% higher, plant growth rate 6–12% higher than control samples) (Mosoarca et al. 2020).

Another study investigated the use of heavy metal treated ceramic powder for cementitious composite production. The unused ceramic powder was found to be an effective substitute for ordinary Portland cement. However, due to the presence of the adsorbed metal ions on the used adsorbent, the use of the loaded adsorbents caused a significant reduction in the rate of strengthening and setting of concrete (Keppert et al. 2018).

Efforts towards industrial applications for CDW-derived adsorbents

Investigation of the feasibility of using CDW-derived adsorbents in large-scale applications is very important to apply these materials in real-world applications. However, the research outcomes in this area are still very sparse for adsorbents derived from CDW.

Ashoori et al. investigated the removal of metal ions, nitrates, and trace organic contaminants using biochar-amended woodchip (composed of different species such as Douglas fir, redwood, and oak) bioreactors in a pilot-scale study. Replicate columns containing woodchips, woodchips and biochar, and wood chips and straw were operated for eight months with saturated continuous flow utilizing water from a watershed that drained an urban area. Then the columns were challenged for a period of five months with continuous exposure to synthetic wastewater containing heavy metals (i.e.those derived from Cd, Cu, Ni, Pb, and Zn). Throughout these experiments, heavy metal removal efficiencies in all treatments were > 80% except for Zn(II) ions. The woodchips-biochar system achieved about 50% removal, while the other systems only removed about 20% of Zn(II) ions (Ashoori et al. 2019).

Another pilot-scale study was conducted using pine bark as a treatment filter for highway runoff for which a synthetic stormwater sample was prepared (Cu, Ni, Pb, and Zn, 1 mg L^{-1} each). The adsorbent (< 4 mm particle size) was placed in the pilot-scale columns with clean quartz sand, and the columns were operated for 2.5 months. Effluent samples were collected biweekly for analysis; the adsorbent showed high performance for metal ion removal, with the highest removal efficiencies observed for Pb(II) and Cu(II) ions (83% and 77%, respectively) (Monrabal-Martinez et al. 2017).

Future research directions

Based on the experimental results of the examined literature, CDW possesses high potential for the adsorption of heavy metal ions. However, when compared to various other adsorbents such as biosorbents and the natural and industrial geomaterials, adsorbents developed from CDW and recycled materials still remain a very poorly studied area (Kumara 2018).

Construction materials vary based on the countries so local variation is strong, and novel adsorbents can be tested directly or after modification for heavy metal treatment. For instance, CDW waste such as glass, plastic waste, and grout can be tested as adsorbents for heavy metal remediation (Girods et al. 2009; Nageeb et al. 2018; Zhang et al. 2020). However, some of these materials may contain hazardous substances due to industrial treatments. Therefore, it is important to characterize these materials carefully prior to adsorption experiments to ensure that hazardous substances do not leach into aqueous solutions, thus defeating the purpose of remediation. Improvements in the adsorption potential of CDW-derived adsorbents can be investigated by mixing CDW with other adsorbents such as natural and industrial geomaterials and biosorbents (Ok et al. 2007; Ashoori et al. 2019).

Another noticeable factor is that most of the studies that investigated the adsorption potential of the CDW are restricted to batch scale analysis (Tables 3 and 4). This operation is scarcely found in real-world applications. Column adsorption studies are more useful for practical applications as a high quantity of wastewater containing a high pollution load can be treated using this technique. Therefore, the adsorption potential of CDW should be investigated further by performing column adsorption analysis. Most of the studies have evaluated the adsorption potential of adsorbents in single-metal ion solution systems. Further analysis should be carried out using multi-metal ion adsorption systems as it is very important for industrial scale applications.

Another important research area that needs further investigation is the application of these adsorbents for the treatment of real wastewater samples, i.e. pilot scale. Very few studies have analysed the adsorption potential of CDW for the treatment of industrial wastewater samples. The adsorbents that have shown high adsorption potential in batch studies and column adsorption studies should be studied further to ascertain their efficacy in industrial wastewater treatment. This is needed as the use of CDW-based adsorbents for water treatment still remains at the laboratory research stage.

In addition, adsorbent regeneration is an important topic for study as it means CDW-derived adsorbents can be reutilized. However, adsorbent regeneration studies are still sparse for the materials derived from CDW such as ceramics, marble powder, and clay-based materials. As stated earlier, the regeneration potential of these adsorbents has been investigated using desorption solvents such as distilled water, acids, bases, or other chemicals albeit with mixed results so lends itself to further study. For instance, the distilled water leaching tests of some CDW-derived adsorbents such as concrete have shown that a very small percentage of the bound metal species are readily soluble (Coleman et al. 2005). Economical and efficient methods should be investigated to recover heavy metal ions from the concentrated metal ion solutions produced after the regeneration process. The utilization of the (heavy metal-laden/spent) adsorbents for other applications is another research area that requires more investigation as this would be an alternative application to attempting to regenerate the spent adsorbents. For instance, wood waste-derived adsorbents treated with heavy metal ions derived from Cu, Zn, and Fe could be investigated for their potential to be applied for soil amendments.

Conclusion

This review presents a comprehensive overview of the application of CDW for heavy metal ion treatment. Researchers have investigated the potential of CDW for heavy metal ion removal either directly (i.e. as-received) or after modifications (chemical modifications, biochar production, activated carbon production). The results of these studies indicate that CDW has the potential for adsorptive removal of heavy metal ions; however, this area is still in its infancy. The nature of the adsorbent, adsorbate, and adsorption conditions such as contact time, metal ion concentration, pH of the solution, and temperature is known to have a significant effect on the adsorption potential of the adsorbent. CDW-derived adsorbents utilize heavy metal ion removal mechanisms such as ion exchange, precipitation, complexation, and electrostatic interactions. After heavy metal ion treatment, the metal ion bearing adsorbent can be investigated for regeneration using desorption solvents such as acids, bases, and distilled water or can be investigated for use in other applications such as fertilizer production and cementitious materials production. The nature of the adsorbent and toxicity of the adsorbed metal ion has to be considered when using the utilized adsorbents in other applications. As we have highlighted in this review, there are still research gaps in this area to be addressed. Therefore, further investigations of these materials are required to effectively use abundantly available CDW materials for wastewater purification in the future.

Declarations

Conflict of interest The authors declare that they have no conflicts of interest.

References

Abegunde SM, Idowu KS, Adejuwon OM, Adeyemi-Adejolu T (2020) A review on the influence of chemical modification on the performance of adsorbents. Res Environ Sustain 1:100001. https://doi.org/10.1016/j.resenv.2020.100001

Abhilash H, McGregor F, Millogo Y, Fabbri A, Séré A, Aubert J-E, Morel J-C (2016) Physical, mechanical and hygrothermal properties of lateritic building stones (LBS) from Burkina Faso. Constr Build Mater 125:731–741. https://doi.org/10.1016/j.conbuildmat.2016.08.082

Adamopoulos S, Foti D, Voulgaridis E, Passialis C (2015) Manufacturing and properties of gypsum-based products with recovered wood and rubber materials. BioResources 10:5573–5585. https://doi.org/10.15376/biores.10.3.5573-5585

Ahalya N, Ramachandra T, Kanamadi R (2003) Biosorption of heavy metals. Res J Chem Environ 7:71–79

Aharoni C, Sideman S, Hoffer E (1979) Adsorption of phosphate ions by collodion-coated alumina. J Chem Technol Biotechnol 29:404–412. https://doi.org/10.1002/jctb.503290703

Ali AF, Abd Ali ZT (2020) Sustainable use of concrete demolition waste as reactive material in permeable barrier for remediation of groundwater: batch and continuous study. J Environ Eng. https://doi.org/10.1061/(ASCE)EE.1943-7870.0001714

Al-Shahrani SS (2014) Treatment of wastewater contaminated with cobalt using Saudi activated bentonite. Alex Eng J 53:205–211. https://doi.org/10.1016/j.aej.2013.10.006

Amarasinghe BM, Williams RA (2007) Tea waste as a low cost adsorbent for the removal of Cu and Pb from wastewater. Chem Eng J 132:299–309. https://doi.org/10.1016/j.cej.2007.01.016

Amin MN, Kaneco S, Kitagawa T, Begum A, Katsumata H, Suzuki T, Ohta K (2006) Removal of arsenic in aqueous solutions by adsorption onto waste rice husk. Ind Eng Chem Res 45:8105–8110. https://doi.org/10.1021/ie060344j

Arabyarmohammadi H, Salarirad MM, Behnamfard A (2014) Characterization and utilization of clay-based construction and demolition wastes as adsorbents for zinc(II) removal from aqueous solutions: an equilibrium and kinetic study. Environ Prog Sustain Energy 33:777–789. https://doi.org/10.1002/ep.11833

Argun ME, Dursun S (2006) Removal of heavy metal ions using chemically modified adsorbents. J Int Environ Appl Sci 1:27–40

Argun ME, Dursun S, Ozdemir C, Karatas M (2007) Heavy metal adsorption by modified oak sawdust: thermodynamics and kinetics. J Hazard Mater 141:77–85. https://doi.org/10.1016/j.jhazmat.2006.06.095

Asgari A, Ghorbanian T, Yousefi N, Dadashzadeh D, Khalili F, Bagheri A, Raei M, Mahvi AH (2017) Quality and quantity of construction and demolition waste in Tehran. J Environ Health Sci Eng 15:1–8. https://doi.org/10.1186/s40201-017-0276-0

Ashoori N, Teixido M, Spahr S, LeFevre GH, Sedlak DL, Luthy RG (2019) Evaluation of pilot-scale biochar-amended woodchip bioreactors to remove nitrate, metals, and trace organic contaminants from urban stormwater runoff. Water Res 154:1–11. https://doi.org/10.1016/j.watres.2019.01.040

Ayawei N, Ebelegi AN, Wankasi D (2017) Modelling and interpretation of adsorption isotherms. J Chem. https://doi.org/10.1155/2017/3039817

Bao T, Chen T, Wille M-L, Chen D, Bian J, Qing C, Wu W, Frost RL (2016) Advanced wastewater treatment with autoclaved aerated concrete particles in biological aerated filters. J Water Process Eng 9:188–194. https://doi.org/10.1016/j.jwpe.2015.11.006

Barkakati P, Begum A, Das ML, Rao PG (2010) Adsorptive separation of Ginsenoside from aqueous solution by polymeric resins: equilibrium, kinetic and thermodynamic studies. Chem Eng J 161:34–45. https://doi.org/10.1016/j.cej.2010.04.018

Baroud TN (2021) The influence of the textural characteristics of the hierarchical porous carbons on the removal of lead and cadmium ions from aqueous solution. Sustainability 13:5790. https://doi.org/10.3390/su13115790

Bartoli M, Giorcelli M, Jagdale P, Rovere M, Tagliaferro A (2020) A review of non-soil biochar applications. Materials 13:261. https://doi.org/10.3390/ma13020261

Bayramoğlu G, Arıca MY (2008) Removal of heavy mercury(II), cadmium(II) and zinc(II) metal ions by live and heat inactivated *Lentinus edodes* pellets. Chem Eng J 143:133–140. https://doi.org/10.1016/j.cej.2008.01.002

Bayuo J, Pelig-Ba KB, Abukari MA (2019) Adsorptive removal of chromium(VI) from aqueous solution unto groundnut shell. Appl Water Sci 9:107. https://doi.org/10.1007/s13201-019-0987-8

Bergsdal H, Bohne RA, Brattebø H (2007) Projection of construction and demolition waste in Norway. J Ind Ecol 11:27–39. https://doi.org/10.1162/jiec.2007.1149

Bibi S, Farooqi A, Hussain K, Haider N (2015) Evaluation of industrial based adsorbents for simultaneous removal of arsenic and fluoride from drinking water. J Clean Prod 87:882–896. https://doi.org/10.1016/j.jclepro.2014.09.030

Blanchard G, Maunaye M, Martin G (1984) Removal of heavy metals from waters by means of natural zeolites. Water Res 18:1501–1507. https://doi.org/10.1016/0043-1354(84)90124-6

Bohart G, Adams E (1920) Some aspects of the behavior of charcoal with respect to chlorine. J Am Chem Soc 42:523–544. https://doi.org/10.1021/ja01448a018

Brunauer S, Emmett PH, Teller E (1938) Adsorption of gases in multimolecular layers. J Am Chem Soc 60:309–319. https://doi.org/10.1021/ja01269a023

Burakov AE, Galunin EV, Burakova IV, Kucherova AE, Agarwal S, Tkachev AG, Gupta VK (2018) Adsorption of heavy metals on conventional and nanostructured materials for wastewater treatment purposes: a review. Ecotoxicol Environ Saf 148:702–712. https://doi.org/10.1016/j.ecoenv.2017.11.034

Caicedo DF, dos Reis GS, Lima EC, De Brum IA, Thue PS, Cazacliu BG, Lima DR, dos Santos AH, Dotto GL (2020) Efficient adsorbent based on construction and demolition wastes functionalized with 3-aminopropyltriethoxysilane (APTES) for the removal ciprofloxacin from hospital synthetic effluents. J Environ Chem Eng. https://doi.org/10.1016/j.jece.2020.103875

Chaplin M (2006) Do we underestimate the importance of water in cell biology? Nat Rev Mol Cell Biol 7:861–866. https://doi.org/10.1038/nrm2021

Chen M, Shafer-Peltier K, Randtke SJ, Peltier E (2018) Competitive association of cations with poly (sodium 4-styrenesulfonate) (PSS) and heavy metal removal from water by PSS-assisted ultrafiltration. Chem Eng J 344:155–164. https://doi.org/10.1016/j.cej.2018.03.054

Chittoo BS, Sutherland C (2020) Column breakthrough studies for the removal and recovery of phosphate by lime-iron sludge: modeling and optimization using artificial neural network and adaptive neuro-fuzzy inference system. Chin J Chem Eng 28:1847–1859. https://doi.org/10.1016/j.cjche.2020.02.022

Colby S, Ortman JM (2015) Projections of the size and composition of the US population: 2014 to 2060

Coleman NJ, Lee WE, Slipper IJ (2005) Interactions of aqueous Cu(II), Zn(II) and Pb(II) ions with crushed concrete fines. J Hazard Mater 121:203–213. https://doi.org/10.1016/j.jhazmat.2005.02.009

Copeland (2020) Types of wood for building projects. https://mtcopeland.com/blog/types-of-wood-for-building-projects/. Accessed 1 July 2021

Davy P, Trompetter W (2018) Heavy metals, black carbon and natural sources of particulate matter in New Zealand, GNS Science Consultancy report, p 81. https://environment.govt.nz/assets/Publications/Files/heavy-metals-black-carbon-and-natural-sources-report.pdf

de Carvalho J, Fungaro DA, Wang SB (2012) Zeolite synthesis from Brazilian coal fly ash for removal of Zn^{2+} and Cd^{2+} from water. Adv Mater Res 356:1900–1908. https://doi.org/10.4028/www.scientific.net/AMR.356-360.1900

De Gisi S, Lofrano G, Grassi M, Notarnicola M (2016) Characteristics and adsorption capacities of low-cost sorbents for wastewater treatment: a review. Sustain Mater Technol 9:10–40. https://doi.org/10.1016/j.susmat.2016.06.002

del Río Merino MM, Izquierdo Gracia P, Weis Azevedo IS (2010) Sustainable construction: construction and demolition waste reconsidered. Waste Manag Res 28:118–129. https://doi.org/10.1177/0734242X09103841

Deng L, Su Y, Su H, Zhu X (2007) Sorption and desorption of lead (II) from wastewater by green algae *Cladophora fascicularis*. J Hazard Mater 143:220–225. https://doi.org/10.1016/j.jhazmat.2006.09.009

Djeribi R, Hamdaoui O (2008) Sorption of copper(II) from aqueous solutions by cedar sawdust and crushed brick. Desalination 225:95. https://doi.org/10.1016/j.desal.2007.04.091

Elboughdiri N (2020) The use of natural zeolite to remove heavy metals Cu (II), Pb (II) and Cd (II), from industrial wastewater. Cogent Eng. https://doi.org/10.1080/23311916.2020.1782623

Elovich SY, Larinov O (1962) Theory of adsorption from solutions of non electrolytes on solid (I) equation adsorption from solutions and the analysis of its simplest form, (II) verification of the equation of adsorption isotherm from solutions. Izv Akad Nauk SSSR Otd Khim Nauk 2:209–216

Elwakeel KZ, Elgarahy AM, Khan ZA, Almughamisi MS, Al-Bogami AS (2020) Perspectives regarding metal/mineral-incorporating materials for water purification: with special focus on Cr(VI) removal. Mater Adv 1:1546–1574. https://doi.org/10.1039/D0MA00153H

Evison DC, Kremer PD, Guiver J (2018) Mass timber construction in Australia and New Zealand—Status, and economic and environmental influences on adoption. Wood Fiber Sci. https://doi.org/10.22382/wfs-2018-046

Fernandez-Luqueno F, López-Valdez F, Gamero-Melo P, Luna-Suárez S, Aguilera-González EN, Martínez AI, García-Guillermo M, Hernández-Martínez G, Herrera-Mendoza R, Álvarez-Garza MA (2013) Heavy metal pollution in drinking water-a global risk for human health: a review. Afr J Environ Sci Technol 7:567–584. https://doi.org/10.5897/AJEST12.197

Freundlich H (1906) Over the adsorption in solution. J Phys Chem 57:1100–1107

Gabr R, Hassan S, Shoreit A (2008) Biosorption of lead and nickel by living and non-living cells of *Pseudomonas aeruginosa* ASU 6a. Int Biodeterior Biodegrad 62:195–203. https://doi.org/10.1016/j.ibiod.2008.01.008

Gambhir RS, Kapoor V, Nirola A, Sohi R, Bansal V (2012) Water pollution: impact of pollutants and new promising techniques in purification process. J Hum Ecol 37:103–109. https://doi.org/10.1080/09709274.2012.11906453

Gao X, Wu L, Xu Q, Tian W, Li Z, Kobayashi N (2018) Adsorption kinetics and mechanisms of copper ions on activated carbons derived from pinewood sawdust by fast H_3PO_4 activation. Environ Sci Pollut Res 25:7907–7915. https://doi.org/10.1007/s11356-017-1079-7

Gęca M, Wiśniewska M, Nowicki P (2022) Biochars and activated carbons as adsorbents of inorganic and organic compounds from multicomponent systems–A review. Adv Colloid Interface Sci. https://doi.org/10.1016/j.cis.2022.102687

Ghazy SE, Gad AH (2014) Lead separation by sorption onto powdered marble waste. Arab J Chem 7:277–286. https://doi.org/10.1016/j.arabjc.2010.10.031

Ghazy SE, Gabr IM, Gad AH (2008) Cadmium (II) sorption from water samples by powdered marble wastes. Chem Speciat Bioavailab 20:249–260. https://doi.org/10.3184/095422908X382152

Ghosal PS, Gupta AK (2017) Determination of thermodynamic parameters from Langmuir isotherm constant-revisited. J Mol Liq 225:137–146. https://doi.org/10.1016/j.molliq.2016.11.058

Girods P, Dufour A, Fierro V, Rogaume Y, Rogaume C, Zoulalian A, Celzard A (2009) Activated carbons prepared from wood particleboard wastes: characterisation and phenol adsorption capacities. J Hazard Mater 166:491–501. https://doi.org/10.1016/j.jhazmat.2008.11.047g

Grace MA, Clifford E, Healy MG (2016) The potential for the use of waste products from a variety of sectors in water treatment processes. J Clean Prod 137:788–802. https://doi.org/10.1016/j.jclepro.2016.07.113

Hai T, Kumara G, Nga T, Giang N, Kawamoto K (2018) Characteristics of cadmium adsorption onto granulated clay brick and laterite, 12th ISE 2018, Tokyo, Japan

Helmer R, Hespanhol I (1997) Water pollution control: a guide to the use of water quality management principles. CRC Press

Herath A, Layne CA, Perez F, Hassan EB, Pittman CU Jr, Mlsna TE (2021) KOH-activated high surface area Douglas Fir biochar

for adsorbing aqueous Cr(VI), Pb(II) and Cd(II). Chemosphere 269:128409. https://doi.org/10.1016/j.chemosphere.2020.128409

Ho H-J, Iizuka A, Shibata E (2020) Chemical recycling and use of various types of concrete waste: a review. J Clean Prod. https://doi.org/10.1016/j.jclepro.2020.124785

Hua T, Haynes R, Zhou Y-F, Boullemant A, Chandrawana I (2015) Potential for use of industrial waste materials as filter media for removal of Al, Mo, As, V and Ga from alkaline drainage in constructed wetlands–adsorption studies. Water Res 71:32–41. https://doi.org/10.1016/j.watres.2014.12.036

Huang Z-H, Zheng X, Lv W, Wang M, Yang Q-H, Kang F (2011) Adsorption of lead(II) ions from aqueous solution on low-temperature exfoliated graphene nanosheets. Langmuir 27:7558–7562. https://doi.org/10.1021/la200606r

Hutson ND, Yang RT (1997) Theoretical basis for the Dubinin-Radushkevitch (D-R) adsorption isotherm equation. Kluwer Academic Publisher

Inglis M (2007) Construction and demolition waste–best practice and cost saving. Ministry for the Environment New Zealand. https://silo.tips/download/construction-and-demolition-waste-best-practice-and-cost-saving-mahara-inglis-bc#

Inyinbor A, Adekola F, Olatunji GA (2016) Kinetics, isotherms and thermodynamic modeling of liquid phase adsorption of Rhodamine B dye onto *Raphia hookerie* fruit epicarp. Water Resour Ind 15:14–27. https://doi.org/10.1016/j.wri.2016.06.001

Ioannidou O, Zabaniotou A (2007) Agricultural residues as precursors for activated carbon production—a review. Renew Sustain Energy Rev 11:1966–2005. https://doi.org/10.1016/j.rser.2006.03.013

Islam R, Nazifa TH, Yuniarto A, Uddin AS, Salmiati S, Shahid S (2019) An empirical study of construction and demolition waste generation and implication of recycling. Waste Manag 95:10–21. https://doi.org/10.1016/j.wasman.2019.05.049

Itodo U, Khan M, Feka D, Ogoh B (2018) Tannery wastewater evaluation and remediation: adsorption of trivalent chromium using commercial and regenerated adsorbents. J Water Technol Treat Meth 1:1–105. https://doi.org/10.31021/jwt.20181105

Jayarama K, Murthy IYLN, Lalhruaitluanga H, Prasad B (2009) Biosorption of lead from aqueous solution by seed powder of *Strychnos potatorum* L. Alex Eng J 71:248–254. https://doi.org/10.1016/j.colsurfb.2009.02.016

Jelić I, Šljivić-Ivanović M, Dimović S, Antonijević D, Jović M, Šerović R, Smičiklas I (2017) Utilization of waste ceramics and roof tiles for radionuclide sorption. Process Saf Environ Prot 105:348–360. https://doi.org/10.1016/j.psep.2016.11.021

Jerman M, Keppert M, Výborný J, Černý R (2013) Hygric, thermal and durability properties of autoclaved aerated concrete. Constr Build Mater 41:352–359. https://doi.org/10.1016/j.conbuildmat.2012.12.036

Jiang M-q, Jin X-y, Lu X-Q, Chen Z-l (2010) Adsorption of Pb(II), Cd(II), Ni(II) and Cu(II) onto natural kaolinite clay. Desalination 252:33–39. https://doi.org/10.1016/j.desal.2009.11.005

Jiang S, Huang L, Nguyen TA, Ok YS, Rudolph V, Yang H, Zhang D (2016) Copper and zinc adsorption by softwood and hardwood biochars under elevated sulphate-induced salinity and acidic pH conditions. Chemosphere 142:64–71. https://doi.org/10.1016/j.chemosphere.2015.06.079

Kandah MI, Meunier J-L (2007) Removal of nickel ions from water by multi-walled carbon nanotubes. J Hazard Mater 146:283–288. https://doi.org/10.1016/j.jhazmat.2006.12.019

Karunanayake AG, Todd OA, Crowley M, Ricchetti L, Pittman CU Jr, Anderson R, Mohan D, Mlsna T (2018) Lead and cadmium remediation using magnetized and nonmagnetized biochar from Douglas fir. Chem Eng J 331:480–491. https://doi.org/10.1016/j.cej.2017.08.124

Keilman N, Pham DQ, Hetland A (2002) Why population forecasts should be probabilistic-illustrated by the case of Norway. Demogr Res 6:409–454. https://doi.org/10.4054/DemRes.2002.6.15

Keppert M, Doušová B, Reiterman P, Koloušek D, Záleská M, Černý R (2018) Application of heavy metals sorbent as reactive component in cementitious composites. J Clean Prod 199:565–573. https://doi.org/10.1016/j.jclepro.2018.07.198

Khan MW (2016) Comparison of construction practices in different countries. https://www.linkedin.com/pulse/comparison-construction-practices-different-countries-khan/. Accessed 26 Aug 2022

Kirchherr J, Reike D, Hekkert M (2017) Conceptualizing the circular economy: an analysis of 114 definitions. Resour Conserv Recycl 127:221–232. https://doi.org/10.1016/j.resconrec.2017.09.005

Koble RA, Corrigan TE (1952) Adsorption isotherms for pure hydrocarbons. Ind Eng Chem 44:383–387. https://doi.org/10.1021/ie50506a049

Kovacova Z, Demcak S, Balintova M, Pla C, Zinicovscaia I (2020) Influence of wooden sawdust treatments on Cu(II) and Zn(II) removal from water. Materials 13:3575. https://doi.org/10.3390/ma13163575

Krishnamoorthy R, Govindan B, Banat F, Sagadevan V, Purushotaman M, Show PL (2019) Date pits activated carbon for divalent lead ions removal. J Biosci Bioeng 128:88–97. https://doi.org/10.1016/j.jbiosc.2018.12.011

Kumara GMP (2018) Reviews on the applicability of construction and demolition waste as low-cost adsorbents to remove heavy metals in wastewater. Int J Geomate. https://doi.org/10.21660/2018.42.7148

Kumara G, Kawamoto K, Saito T, Hamamoto S, Asamoto S (2019) Evaluation of autoclaved aerated concrete fines for removal of Cd(II) and Pb(II) from wastewater. J Environ Eng 145:04019078. https://doi.org/10.1061/(ASCE)EE.1943-7870.0001597

Labidi N (2008) Removal of mercury from aqueous solutions by waste brick. Int J Environ Res 2:275–278. https://doi.org/10.22059/IJER.2010.204

Lagergren SK (1898) About the theory of so-called adsorption of soluble substances. Sven Vetenskapsakad Handingarl 24:1–39

Langmuir I (1918) The adsorption of gases on plane surfaces of glass, mica and platinum. J Am Chem Soc 40:1361–1403. https://doi.org/10.1021/ja02242a004

Lata S, Singh P, Samadder S (2015) Regeneration of adsorbents and recovery of heavy metals: a review. Int J Environ Sci Technol 12:1461–1478. https://doi.org/10.1007/s13762-014-0714-9

Leng Y, Guo W, Su S, Yi C, Xing L (2012) Removal of antimony(III) from aqueous solution by graphene as an adsorbent. Chem Eng J 211:406–411. https://doi.org/10.1016/j.cej.2012.09.078

Liu P, Borrell PF, Božič M, Kokol V, Oksman K, Mathew AP (2015) Nanocelluloses and their phosphorylated derivatives for selective adsorption of Ag^+, Cu^{2+} and Fe^{3+} from industrial effluents. J Hazard Mater 294:177–185. https://doi.org/10.1016/j.jhazmat.2015.04.001

Lu C, Chiu H (2006) Adsorption of zinc(II) from water with purified carbon nanotubes. Chem Eng Sci 61:1138–1145. https://doi.org/10.1016/j.ces.2005.08.007

Maji SK, Pal A, Pal T, Adak A (2007) Modeling and fixed bed column adsorption of As(V) on laterite soil. J Environ Sci Health A 42:1585–1593. https://doi.org/10.1080/10934520701517713

McGuigan CF, Hamula CL, Huang S, Gabos S, Le XC (2010) A review on arsenic concentrations in Canadian drinking water. Environ Rev 18:291–307. https://doi.org/10.1139/A10-012

McKeever DB, Elling J (2015) Wood products and other building materials used in new residential construction in the United States. APA-The Engineered Wood Assoc., pp 1–131

Menegaki M, Damigos D (2018) A review on current situation and challenges of construction and demolition waste management. Curr Opin Green Sustain Chem 13:8–15. https://doi.org/10.1016/j.cogsc.2018.02.010

Mohiuddin KM, Ogawa YZ, Zakir HM, Otomo K, Shikazono N (2011) Heavy metals contamination in water and sediments of an urban river in a developing country. Int J Environ Sci Technol 100:723–736. https://doi.org/10.1007/bf03326257

Monrabal-Martinez C, Ilyas A, Muthanna TM (2017) Pilot scale testing of adsorbent amended filters under high hydraulic loads for highway runoff in cold climates. Water 9:230. https://doi.org/10.3390/w9030230

Mosoarca G, Vancea C, Popa S, Boran S, Tanasie C (2020) A green approach for treatment of wastewater with manganese using wood ash. J Chem Technol Biotechnol 95:1781–1789. https://doi.org/10.1002/jctb.6376

Murugesan GS, Sathishkumar M, Swaminathan K (2006) Arsenic removal from groundwater by pretreated waste tea fungal biomass. Bioresour Technol 97:483–487. https://doi.org/10.1016/j.biortech.2005.03.008

Nageeb R, Gad A, Abdeldaiem A (2018) Preparation of low-cost adsorbent from waste glass for the removal of heavy metals from polluted water. J Ind Environ Chem 2:7–18

Nagy B, Mânzatu C, Măicăneanu A, Indolean C, Silaghi-Dumitrescu L, Majdik C (2014) Effect of alkaline and oxidative treatment on sawdust capacity to remove Cd(II) from aqueous solutions: FTIR and AFM study. J Wood Chem Technol 34:301–311. https://doi.org/10.1080/02773813.2013.875040

Ndukwe I, Yuan Q (2016) Drywall (gyproc plasterboard) recycling and reuse as a compost-bulking agent in Canada and North America: a review. Recycling 1:311–320. https://doi.org/10.3390/recycling1030311

Obayomi K, Bello J, Yahya MD, Chukwunedum E, Adeoye J (2020) Statistical analyses on effective removal of cadmium and hexavalent chromium ions by multiwall carbon nanotubes (MWCNTs). Heliyon 6:e04174. https://doi.org/10.1016/j.heliyon.2020.e04174

Ok YS, Yang JE, Zhang Y-S, Kim S-J, Chung D-Y (2007) Heavy metal adsorption by a formulated zeolite-Portland cement mixture. J Hazard Mater 147:91–96. https://doi.org/10.1016/j.jhazmat.2006.12.046

Okazaki K, Pribadi KS, Kusumastuti D, Saito T (2012) Comparison of current construction practices of non-engineered buildings in developing countries. In: Fifthteenth world conference on earthquake engineering, Lisbon

Olalekan A, Dada A, Okewale A (2013) Comparative adsorption isotherm study of the removal of Pb(II) and Zn(II) onto agricultural waste. Res J Chem Environ Sci 1:22–27

Ouyang D, Zhuo Y, Hu L, Zeng Q, Hu Y, He Z (2019) Research on the adsorption behavior of heavy metal ions by porous material prepared with silicate tailings. Minerals 9:291. https://doi.org/10.3390/min9050291

Oyeku OTE (2010) Heavy metal contamination of groundwater resources in a Nigerian urban settlement. Afr J Environ Sci Technol 4:201–214

Özdes D, Yildirim İ, Duran C (2020) Adsorptive removal of Cr(VI) ions from aqueous solutions by H_2SO_4 modified oak (*Quercus* L.) sawdust. Turk J Anal Chem 2:7–14

Palma G, Freer J, Baeza J (2003) Removal of metal ions by modified *Pinus radiata* bark and tannins from water solutions. Water Res 37:4974–4980. https://doi.org/10.1016/j.watres.2003.08.008

Passos J, Alves O, Brito P (2020) Management of municipal and construction and demolition wastes in Portugal: future perspectives through gasification for energetic valorisation. Int J Environ Sci Technol. https://doi.org/10.1007/s13762-020-02656-6

Peng H, Gao P, Chu G, Pan B, Peng J, Xing B (2017) Enhanced adsorption of Cu(II) and Cd(II) by phosphoric acid-modified biochars. Environ Pollut 229:846–853. https://doi.org/10.1016/j.envpol.2017.07.004

Peter A, Chabot B, Loranger E (2021) Enhanced activation of ultrasonic pre-treated softwood biochar for efficient heavy metal removal from water. J Environ Manag. https://doi.org/10.1016/j.jenvman.2021.112569

Poo K-M, Son E-B, Chang J-S, Ren X, Choi Y-J, Chae K-J (2018) Biochars derived from wasted marine macro-algae (*Saccharina japonica* and *Sargassum fusiforme*) and their potential for heavy metal removal in aqueous solution. J Environ Manag 206:364–372. https://doi.org/10.1016/j.jenvman.2017.10.056

Poorkarimi S, Hallajisani A, Ghorbanian SA, Bagheri N, Shahbeig H (2013) A new adsorption isotherm model of aqueous solutions on granular activated carbon. World J Model Simul 9:243–254

Putra WP, Mohamed A, Hashim M, Isa IM (2014) Biosorption of Cu(II), Pb(II) and Zn(II) Ions from aqueous solutions using selected waste materials: adsorption and characterisation studies. J Encapsulation Adsorpt Sci 4:25–35. https://doi.org/10.4236/jeas.2014.41004

Qiu B, Tao X, Wang H, Li W, Ding X, Chu H (2021) Biochar as a low-cost adsorbent for aqueous heavy metal removal: a review. J Anal Appl Pyrolysis. https://doi.org/10.1016/j.jaap.2021.105081

Radke C, Prausnitz J (1972) Adsorption of organic solutes from dilute aqueous solution of activated carbon. Ind Eng Chem Fundam 11:445–451. https://doi.org/10.1021/i160044a003

Radushkevich M (1947) The equation of the characteristic curve of the activated charcoal USSR. Phys Chem Sect 55:331–333

Rafatullah M, Sulaiman O, Hashim R, Ahmad A (2009) Adsorption of copper(II), chromium(III), nickel(II) and lead(II) ions from aqueous solutions by meranti sawdust. J Hazard Mater 170:969–977. https://doi.org/10.1016/j.jhazmat.2009.05.066

Rafatullah M, Sulaiman O, Hashim R, Ahmad A (2012) Removal of cadmium(II) from aqueous solutions by adsorption using meranti wood. Wood Sci Technol 46:221–241. https://doi.org/10.1007/s00226-010-0374-y

Rahmatnia MA, Nouralishahi A, Baheddini M, Hallajisani A (2021) Alkali activated cedar wood as an efficient adsorbent for Pb^{2+} removal from aqueous solutions: optimization, kinetic and thermodynamic study. Sci Iran. https://doi.org/10.24200/SCI.2021.55733.4379

Ramage MH, Burridge H, Busse-Wicher M, Fereday G, Reynolds T, Shah DU, Wu G, Yu L, Fleming P, Densley-Tingley D (2017) The wood from the trees: the use of timber in construction. Renew Sustain Energy Rev 68:333–359. https://doi.org/10.1016/j.rser.2016.09.107

Rasool A, Xiao T, Farooqi A, Shafeeque M, Masood S, Ali S, Fahad S, Nasim W (2016) Arsenic and heavy metal contaminations in the tube well water of Punjab, Pakistan and risk assessment: a case study. Ecol Eng 95:90–100. https://doi.org/10.1016/j.ecoleng.2016.06.034

Ray S, Gusain R, Kumar N (2020) Adsorption in the context of water purification. Carbon nanomaterial-based adsorbents for water purification. Elsevier, pp 67–100

Redlich O, Peterson DL (1959) A useful adsorption isotherm. J Phys Chem 63:1024–1024. https://doi.org/10.1021/j150576a611

Riahi K, Chaabane S, Thayer BB (2017) A kinetic modeling study of phosphate adsorption onto *Phoenix dactylifera* L. date palm fibers in batch mode. J Saudi Chem Soc 21:S143–S152. https://doi.org/10.1016/j.jscs.2013.11.007

Risse M, Weber-Blaschke G, Richter K (2019) Eco-efficiency analysis of recycling recovered solid wood from construction into laminated timber products. Sci Total Environ 661:107–119. https://doi.org/10.1016/j.scitotenv.2019.01.117

Rong J, Zhao Z, Jing Z, Zhang T, Qiu F, Xu J (2017) High-specific surface area hierarchical Al_2O_3 carbon fiber based on a waste paper fiber template: preparation and adsorption for iodide ions. J Wood Chem Technol 37:485–492. https://doi.org/10.1080/02773813.2017.1347684

Salazar-Rabago J, Leyva-Ramos R (2016) Novel biosorbent with high adsorption capacity prepared by chemical modification of white pine (*Pinus durangensis*) sawdust. Adsorption of Pb (II) from aqueous solutions. J Environ Manag 169:303–312. https://doi.org/10.1016/j.jenvman.2015.12.040

Salim M, Munekage Y (2009a) Lead removal from aqueous solution using silica ceramic: adsorption kinetics and equilibrium studies. Int J Chem 1:23–30. https://doi.org/10.5539/ijc.v1n1p23

Salim M, Munekage Y (2009b) Removal of arsenic from aqueous solution using silica ceramic: adsorption kinetics and equilibrium studies. Int J Environ Res 3:13–22. https://doi.org/10.22059/IJER.2009.8

Schwerin DE, Cavalline TL, Weggel DC (2013) Use of recycled brick masonry aggregate and recycled brick masonry aggregate concrete in sustainable construction. J Const Eng Manag 3:28–34. https://doi.org/10.6106/JCEPM.2013.3.1.028

Šćiban M, Klašnja M, Škrbić B (2006) Modified softwood sawdust as adsorbent of heavy metal ions from water. J Hazard Mater 136:266–271. https://doi.org/10.1016/j.jhazmat.2005.12.009

Selim AQ, Sellaoui L, Ahmed SA, Mobarak M, Mohamed EA, Lamine AB, Erto A, Bonilla-Petriciolet A, Seliem MK (2019) Statistical physics-based analysis of the adsorption of Cu^{2+} and Zn^{2+} onto synthetic cancrinite in single-compound and binary systems. J Environ Chem Eng 7:103217. https://doi.org/10.1016/j.jece.2019.103217

Senthil Kumar P, Sai Deepthi ASL, Bharani R, Prabhakaran C (2013) Adsorption of Cu(II), Cd(II) and Ni(II) ions from aqueous solution by unmodified *Strychnos potatorum* seeds. Eur J Environ Civ 17:293–314. https://doi.org/10.1080/19648189.2013.785983

Sfaksi Z, Azzouz N, Abdelwahab A (2014) Removal of Cr(VI) from water by cork waste. Arab J Chem 7:37–42. https://doi.org/10.1016/j.arabjc.2013.05.031

Singh S, Kumar M (2006) Heavy metal load of soil, water and vegetables in peri-urban Delhi. Environ Monit Assess 120:79–91. https://doi.org/10.1007/s10661-005-9050-3

Singh S, Ma L, Harris W (2001) Heavy metal interactions with phosphatic clay: sorption and desorption behavior. J Environ Qual 30:1961–1968. https://doi.org/10.2134/jeq2001.1961

Tchobanoglous G, Theisen H, Vigil S (1993) Integrated solid waste management: engineering principles and management lssues. McGraw-Hill, New York

Tomczyk A, Sokołowska Z, Boguta P (2020) Biochar physico-chemical properties: pyrolysis temperature and feedstock kind effects. Rev Environ Sci Biotechnol 19:191–215. https://doi.org/10.1007/s11157-020-09523-3

Tonini M, Parente J, Pereira M (2018) Global assessment of land cover changes and rural-urban interface in Portugal. Nat Hazards Earth Syst Sci Discuss. https://doi.org/10.5194/nhess-2017-359

Townsend T, Wilson C, Beck B (2014) The benefits of construction and demolition materials recycling in the United States. https://nrcne.org/wp-content/uploads/2019/12/cdra_benefits_of_cd_recycling_final_revised_2017.pdf

Tsai W, Chang C, Lee S (1997) Preparation and characterization of activated carbons from corn cob. Carbon 35:1198–1200

Tsekova K, Todorova D, Dencheva V, Ganeva S (2010) Biosorption of copper(II) and cadmium(II) from aqueous solutions by free and immobilized biomass of *Aspergillus niger*. Bioresour Technol 101:1727–1731. https://doi.org/10.1016/j.biortech.2009.10.012

Tuomikoski S, Runtti H, Romar H, Lassi U, Kangas T (2021) Multiple heavy metal removal simultaneously by a biomass-based porous carbon. Water Environ Res. https://doi.org/10.1002/wer.1514

Varol M, Şen B (2012) Assessment of nutrient and heavy metal contamination in surface water and sediments of the upper Tigris River, Turkey. CATENA 92:1–10. https://doi.org/10.1016/j.catena.2011.11.011

Vengris T, Binkien R, Sveikauskait A (2001) Nickel, copper and zinc removal from waste water by a modified clay sorbent. Appl Clay Sci 18:183–190. https://doi.org/10.1016/S0169-1317(00)00036-3

WHO (2011) Guidelines for drinking-water quality. WHO Chron 38:104–108

Wong Y, Szeto Y, Cheung W, McKay G (2003) Equilibrium studies for acid dye adsorption onto chitosan. Langmuir 19:7888–7894. https://doi.org/10.1021/la030064y

Wu J, Ren D, Zhang X, Chen Z, Zhang S, Li S, Fu L (2019) The adsorption properties of biochar derived from woody plants or bamboo for cadmium in aqueous solution. Desalin Water Treat 160:268–275. https://doi.org/10.5004/dwt.2019.24174

Yan G, Viraraghavan T, Chen M (2001) A new model for heavy metal removal in a biosorption column. Adsorp Sci Technol 19:25–43. https://doi.org/10.1260/0263617011493953

Yokogawa Y, Yamauchi R, Saito A, Yamato Y, Toma T (2017) Kinetic modelling of cytochrome c adsorption on SBA-15. Biomed Mater Eng 28:37–46. https://doi.org/10.3233/BME-171654

Yoo J, Shin H, Ji S (2018) Evaluation of the applicability of concrete sludge for the removal of Cu, Pb, and Zn from contaminated aqueous solutions. Metals 8:666. https://doi.org/10.3390/met8090666

Yuan H, Lu T, Wang Y, Chen Y, Lei T (2016) Sewage sludge biochar: nutrient composition and its effect on the leaching of soil nutrients. Geoderma 267:17–23. https://doi.org/10.1016/j.geoderma.2015.12.020

Zhang X, Guo S, Liu J, Zhang Z, Song K, Tan C, Li H (2019) A study on the removal of copper(II) from aqueous solution using lime sand bricks. Appl Sci 9:670. https://doi.org/10.3390/app9040670

Zhang H, Pap S, Taggart MA, Boyd KG, James NA, Gibb SW (2020) A review of the potential utilisation of plastic waste as adsorbent for removal of hazardous priority contaminants from aqueous environments. Environ Pollut 258:113698. https://doi.org/10.1016/j.envpol.2019.113698